Tectonics

RESEARCH ARTICLE
10.1029/2022TC007618

Present-Day Caribbean-North American Oblique Convergence Through the Ocoa-Bonao-La Guacara Fault Zone, Southern Central Hispaniola: A Transition Zone Between Oceanic Subduction and Arc-Oceanic Plateau Collision

J. Escuder-Viruete[1], F. J. Fernández[2], F. Pérez Valera[3], and A. Medialdea[4]

[1]Instituto Geológico y Minero España, CSIC, C. La Calera 1, Madrid, Spain, [2]Departamento de Geología, Universidad de Oviedo. C. Jesús Arias de Velasco, Oviedo, Spain, [3]Departamento de Ciencias de la Tierra y del Medio Ambiente, Universidad de Alicante, Sant Vicent de Raspeig, Alicante, Spain, [4]Centro Nacional de Investigación sobre la Evolución Humana (CENIEH), Paseo Sierra Atapuerca 3, Burgos, Spain

Abstract According to GPS measurements, the Caribbean plate is moving east-northeastward relative to the North American plate at a rate of ~20 mm/a. This oblique motion is partly accommodated in southern Hispaniola by northward underthrusting/subduction bellow the Muertos submerged accretionary prism and the Peralta fold-and-thrust belt. This work investigates the active transition zone that connects Muertos and Peralta: the Ocoa-Bonao-La Guacara fault zone (OBFZ). Combined detailed structural analysis at macroscopic and mesoscopic scales, regional magnetic data and seismicity analysis, geomorphic observations, fault-slip data inversion and geochronology of Quaternary deposits allow to establish the deformation pattern for the OBFZ along southern central Hispaniola. Distinct tectonic regimes have occurred successively in the Neogene, within a consistent regional NE-trending horizontal shortening: (a) a lower Miocene to Early Pleistocene D1 regime characterized by SW-directed thrusting that homogeneously affects the region; and (b) an Early/Middle Pleistocene to Holocene D2 regime of strike-slip to transpressional faulting mainly located along the OBFZ. The change is coeval with the tectonic indentation of the Beata Ridge in the back-arc region of the Hispaniola microplate. Finally, a Late Pleistocene to Holocene D3 extensional regime has a local development around the Ocoa Bay. Part of the present-day stress-field induced by the Beata Ridge collision is accommodated by the OBFZ within the Hispaniola microplate. This fault zone defines the onland transition between oceanic subduction and arc-oceanic plateau collision. Due to its length and potential to generate large earthquakes, the OBFZ must be considered in the regional seismic hazard assessment.

Key Points:

- The Ocoa-Bonao-La Guacara fault zone (OBFZ) is composed of four segments with specific kinematics
- The OBFZ records an Early to Middle Pleistocene to Holocene regime of strike-slip to transpressional faulting
- The OBFZ defines the active transition between oceanic subduction and arc-oceanic plateau collision

Supporting Information:

Supporting Information may be found in the online version of this article.

Correspondence to:

J. Escuder-Viruete,
javier.escuder@csic.es

Citation:

Escuder-Viruete, J., Fernández, F. J., PérezValera, F., & Medialdea, A. (2023). Present-day Caribbean-North American oblique convergence through the Ocoa-Bonao-La Guacara fault zone, southern central Hispaniola: A transition zone between oceanic subduction and arc-oceanic plateau collision. *Tectonics*, *42*, e2022TC007618. https://doi.org/10.1029/2022TC007618

Received 30 SEP 2022
Accepted 30 MAR 2023

Author Contributions:

Conceptualization: J. Escuder-Viruete, F. J. Fernández, F. Pérez Valera, A. Medialdea
Formal analysis: J. Escuder-Viruete, F. J. Fernández, F. Pérez Valera, A. Medialdea
Investigation: J. Escuder-Viruete, F. J. Fernández, F. Pérez Valera, A. Medialdea
Methodology: J. Escuder-Viruete
Project Administration: J. Escuder-Viruete
Writing – original draft: J. Escuder-Viruete

1. Introduction

The current ENE-directed convergence of ~20 mm/a between the Caribbean and North American plates in southern Hispaniola (Dominican Republic and Haiti; Figure 1) accommodates partly by northward underthrusting/subduction below the Muertos accretionary prism. To the W, convergence adjusts partially by folding and faulting related to collision between the Beata Ridge, a large bathymetric feature on the Caribbean plate, and the back-arc edge of the Caribbean island-arc (Hernáiz-Huerta, Díaz De Neira, García Senz, Deschamps, Lopera, et al., 2007; Hernáiz-Huerta, Díaz De Neira, García Senz, Deschamps, Genna, et al., 2007; Hernáiz-Huerta & Pérez-Estaún, 2002; Heubeck & Mann, 1991; Mann, Draper, & Lewis, 1991; Mann, McLaughlin, and Cooper, 1991; Mercier de Lépinay, 1987).

Previous tectonic models by Matthews & Holcombe (1976), Ladd et al. (1981) and Biju-Duval et al. (1982) for the Neogene evolution of southern Hispaniola, envisioned the Beata Ridge as a simple right-lateral strike-slip fault that accommodated the relative motion between an area of NE-directed crustal shortening in central Hispaniola and an area of underthrusting along the Muertos trench. Mercier de Lepinay et al. (1988) described a Neogene collision between the Beata Ridge and southern Hispaniola margin based on marine geophysical surveys and field data. The collision would give rise to the structure of the Southern Peninsula of Hispaniola (composed by the Massifs de Hotte-Selle in Haiti and Sierra de Bahoruco in the Dominican Republic), as a collage of basaltic slices of the ridge sweeping eastward the southern boundary of the north Caribbean orogenic belt.

Witschard & Dolan (1990), Dolan et al. (1991), and Heubeck and Mann (1991) recognized the localized NE-directed indentation of the thickened crust of the Beata Ridge along a width of about 50 km on southern

Writing – review & editing: F. J. Fernández, F. Pérez Valera, A. Medialdea

Hispaniola in the late Pliocene to present-day. The indentation model is supported by the arcuate trend and apparent counterclockwise rotation of fold structures west of the Ocoa Bay (Sierra de Martín García), and clockwise rotation of fold and thrust structures east of the Ocoa Bay (Sierra de Número). These regional structures rotated together during the NE-directed displacement of the northern edge of the Beata Ridge relative to the surrounding landmass of Hispaniola. For this time and based on geochemical and geochronological data, the Cretaceous basalts that form the basement of the Southern Peninsula were defined as an uplifted/accreted fragment of the Caribbean Large Igneous Province (CLIP), which continues southward through the Beata Ridge (Dürkefälden et al., 2019; Escuder-Viruete, Joubert, et al., 2016; Lewis & Draper, 1990; Révillon et al., 2000; Sen et al., 1988; Sinton et al., 1998).

Later, Hernaiz Huerta & Pérez-Estaún (2002), Hernáiz-Huerta, Díaz De Neira, García Senz, Deschamps, Genna, et al. (2007), and Pérez Valera (2010) attribute the right and left-lateral strike-slip faults and drag effects on the previous fold and thrust structures, observed respectively on the eastern and western sides of the Ocoa Bay, to the Plio-Quaternary indentation of the southern margin of Hispaniola by the NE-directed displacement of the Beata Ridge. Based on swath bathymetry and seismic reflection data of the offshore southern slope of the Dominican Republic, Granja Bruña et al. (2014) also propose the collision and impingement of the thickened crust of the Beata ridge into south Hispaniola. For these authors, however, the fault zone that limits the Sierra de Bahoruco to the E and extends to the NE in the eastern Ocoa Bay plays a dominant role. The Bahoruco fault zone is an old normal fault that acts as a passive tear fault accommodating the sharp along-strike transition from thrusting in the Muertos margin to collision and uplift in the Bahoruco Peninsula. Following the ideas of Mercier de Lepinay et al. (1988), these authors propose a collision accommodation by E-W trending left-lateral transpression, accretion and counterclockwise rotation of blocks of the Beata Ridge along the whole Southern Peninsula of Hispaniola. The E-W trending, left-lateral Enriquillo-Plantain Garden fault zone (EPGFZ) is part of the transpressive deformation in this tectonic context.

This paper presents new structural data, fault-slip data inversion and optically stimulated luminescence (OSL) geochronology to better understand the regional process of collision between the Beata Ridge and the back-arc margin of the Caribbean island-arc. In particular, the role played by the Ocoa-Bonao-La Guacara fault zone (OBFZ), which is an active, NNE to NE-striking large-scale fault system that crosses the southern central sector of Hispaniola in the Dominican Republic along more than 250 km. These data have allowed: (a) to establish for the first time the neotectonic deformation pattern of the OBFZ, particularly its fault segmentation, based on structural and geomorphic field observations, complemented with the analysis of satellite image, regional magnetic data and seismicity; (b) to determine the kinematics of the fault system by observation of mesoscopic faults in late Cretaceous to Pleistocene rocks; (c) to determine the Pliocene to present-day evolution of the stress regime within and around the OBFZ based on fault-slip data; (d) to constrain the age of the OBFZ by dating related Quaternary deposits; and (e) to preliminarily assess the seismic potential of the OBFZ. Finally, in conjunction with published regional data, we propose a geodynamic reconstruction for the arc-oceanic plateau collision in southern Hispaniola during the Quaternary.

2. Geological Setting

2.1. From Intra-Oceanic Subduction to Arc-Continent Collision in the Northern Caribbean Plate

The geology of Hispaniola is the result of the SW-directed Cretaceous subduction to final oblique collision in the Eocene of the Caribbean intra-oceanic arc with the southern continental margin of North America (Escuder-Viruete, Pérez-Estaún, Gabites, & Suárez-Rodríguez, 2011; Escuder-Viruete, Pérez-Estaún, Gabites, & Suárez-Rodríguez, 2011; Escuder-Viruete, Súarez, et al., 2016; Escuder-Viruete et al., 2013; Draper et al., 1994; Mann, Draper, & Lewis, 1991; Pérez-Estaún et al., 2007). The high-P mélanges and ophiolites in northern Hispaniola indicate that an intermediate proto-Caribbean oceanic basin subducted since the early Cretaceous (Draper & Nagle, 1991; Escuder-Viruete & Pérez-Estaún, 2013; Krebs et al., 2011). The magmatic activity in the Caribbean upper plate is represented by Aptian to the lower Eocene volcanic and plutonic rocks (Escuder-Viruete et al., 2006, 2014, 2022; Kesler et al., 2005). The arc-related rocks are covered by middle to upper Eocene to lower Miocene sedimentary rocks. This cover post-dates the magmatic island-arc activity and records the oblique arc-continent collision in northern Hispaniola, as well as intra- and back-arc deformation by back-thrusting in the central and southern areas of the island (Mann, Draper, & Lewis, 1991; Mann, McLaughlin, and Cooper, 1991; Mann et al., 1995; Pérez-Estaún et al., 2007). The main consequence of the arc-continent collision and the

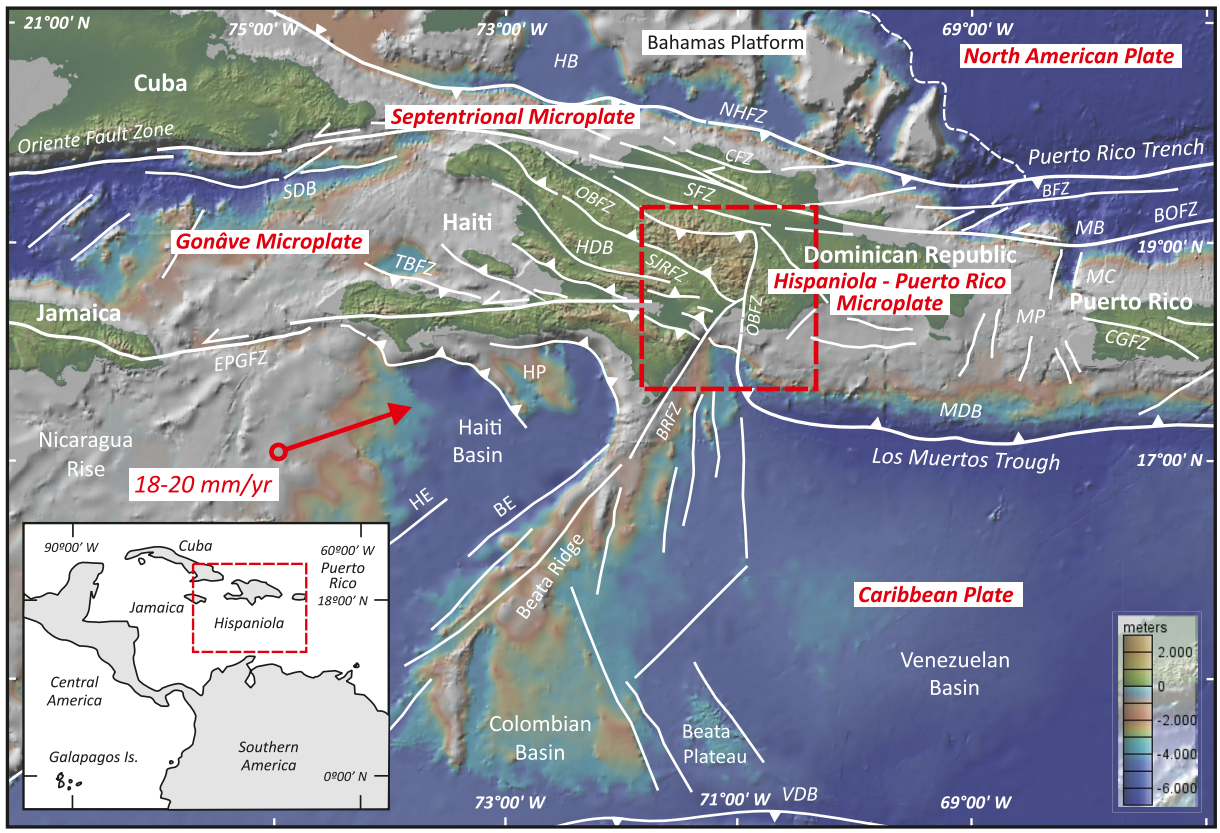

Figure 1. Map of the northeast edge of the Caribbean Plate showing the location of plate and microplate boundaries, as well as the main tectonic structures. The red arrow defines the movement vector of 18–20 mm/a in the direction N070ºE of the Caribbean Plate with respect to the North American Plate (mod. Mann et al., 2002). Relief in color scale has been made from the GMRT synthesis data set (Ryan et al., 2009) with GeoMapApp (www.geomapapp.org). The discontinuous red rectangle defines the situation of the study area in central and southern Dominican Republic (Figure 2). Diagram on the bottom left shows the location of Hispaniola (Dominican Republic and Haiti) in the Caribbean region. BE, Beata Escarpement; BFZ, Bowin fault zone; BRFZ, Beata Ridge fault zone; CFZ, Camú fault zone; CGFZ, Cerro Goden fault zone; EPGFZ, Enriquillo-Platain Garden fault zone; HB, Hispaniola Basin; HDB; Haiti Deformed Belt; HE, Hess Escarpement; MC, Mona Canyon; MDB, Muertos Deformed Belt; MP, Mona Passage; NHFZ, North Hispaniola fault zone; HP, Haiti Plateau; OBFZ, Ocoa-Bonao-La Guacara fault zone; SFZ, Septentrional fault zone; SJPFZ, San Juan-Pozos fault zone; VDB, Venezuela Deformed Belt; TBFZ; Trois Baies fault zone.

transfer of deformation to the back-arc region is the subduction polarity reversal or back-thrusting with renewed subduction beginning along a new SW-facing subduction zone (Kroehler et al., 2011).

2.2. From Back-Thrusting to Partitioned Transpression in Hispaniola

The tectonic regime evolved from oblique convergence to crustal-scale strike-slip faulting and eastward escape of the Caribbean plate toward a collision-free side in the Atlantic Ocean since the middle Miocene (Mann, Draper, & Lewis, 1991; Mann, McLaughlin, and Cooper, 1991; Mann et al., 2002). Still active in northern Hispaniola, this tectonic regime gave rise to transpressive tectonics, usually partitioned into thrust and strike-slip faults, tectonic disruption of the Caribbean-North America plate boundary zone, and lateral escape of blocks (Calais & Mercier de Lépinay, 1991; Calais et al., 1992; Dolan et al., 1998; Escuder-Viruete & Pérez, 2020; Escuder-Viruete et al., 2020; Mann, Draper, & Lewis, 1991; Mann, McLaughlin, & Cooper, 1991; Mann et al., 1995, 1998, 2002; Rodríguez-Zurrunero et al., 2019). Two distinct strike-slip fault systems are present in the Hispaniola island marked by shallow seismicity (Figure 1; Mann, Draper, & Lewis, 1991; Mann, McLaughlin, and Cooper, 1991): the Septentrional fault zone (SFZ) and the Enriquillo-Plantain Garden fault zone (EPGFZ). Two thrust fault systems occur in offshore areas marked by intermediate to deep seismicity: the Northern Hispaniola fault zone (NHFZ; also called northern Hispaniola deformed belt); and the Muertos Trough (MT; also called Muertos deformed belt). The NHFZ constitutes the S-dipping collisional contact between northern Hispaniola and the Bahamas platform of the North America plate, and the MT is the N-dipping subduction and/or underthrusting contact between southern Hispaniola and the Caribbean oceanic crust. Displacements along these fault systems

10.1029/2022TC007618

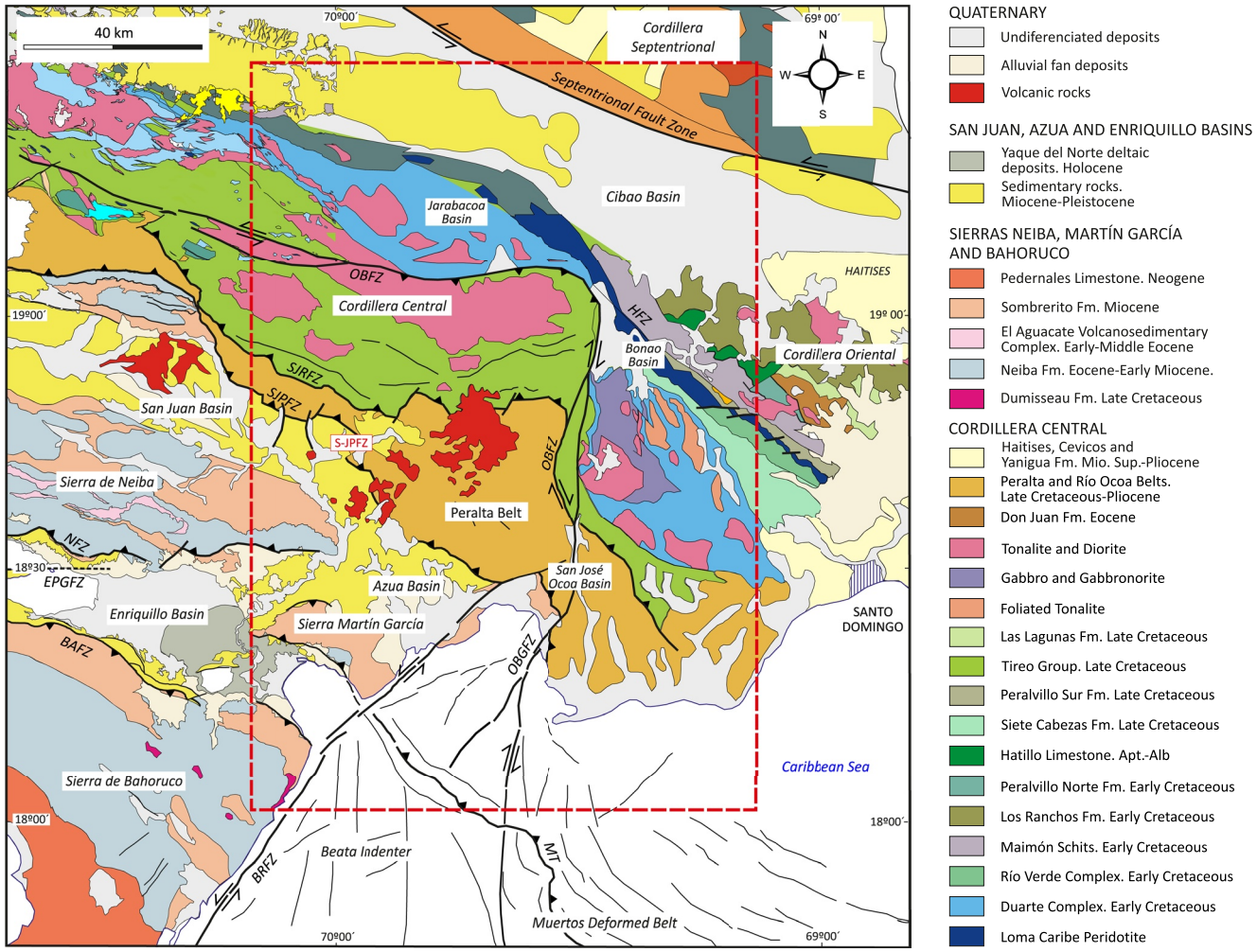

Figure 2. Schematic geologic map of southern Hispaniola (modified from the SYSMIN Project; Pérez-Estaún et al., 2007). HFZ, Hispaniola fault zone; NFZ, Neiba fault zone; SJRFZ, San José-Restauración fault zone; SJPFZ, San Juan-Pozos fault zone. Rest of acronyms as in Figure 1. The box with the discontinuous red line marks the situation illustrated in Figure 3.

have generated several major, destructive historical earthquakes; therefore, they represent a critical seismic hazard to the densely populated island of Hispaniola (Prentice et al., 2010; ten Brink et al., 2011; Bakun et al., 2012).

2.3. The Hispaniola-Puerto Rico Microplate

Several microplates or tectonic blocks limited by fault zones have been distinguished in the northeast Caribbean region (Benford et al., 2012; Calais et al., 2016; Manaker et al., 2008; Mann, Draper, & Lewis, 1991, 1995, 2002; Rodríguez-Zurrunero et al., 2019; Symithe et al., 2015). These microplates are (Figure 1): Gonâve, Septentrional (or North Hispaniola) and Hispaniola-Puerto Rico. The Ocoa-Bonao-La Guacara fault zone is located in the Hispaniola-Puerto Rico microplate (Figure 2). The Hispaniola-Puerto Rico microplate is an arc crust block, limited northward by the SFZ and southward by the MT. To the E, the microplate is subdivided into the Hispaniola and Puerto Rico-Virgin Islands blocks at the Mona Rift (Mann et al., 2002). To the W, the border between the Hispaniola block and Gonâve microplate is located in the San Juan-Los Pozos fault zone (SJPFZ). However, some researchers place it in the Haitian deformed belt (Benford et al., 2012), the Plateau Central-San Juan Basin in southern Hispaniola (Calais et al., 2016), or as a broad zone of difuse deformation between both domains (Symithe et al., 2015). Seismic tomography across the MT shows N-dipping Caribbean lithosphere to depths of around 100 km below the Hispaniola block (van Benthem et al., 2013), according to regional seismicity and seismic profiles (Granja Bruña et al., 2009, 2014; Symithe et al., 2015).

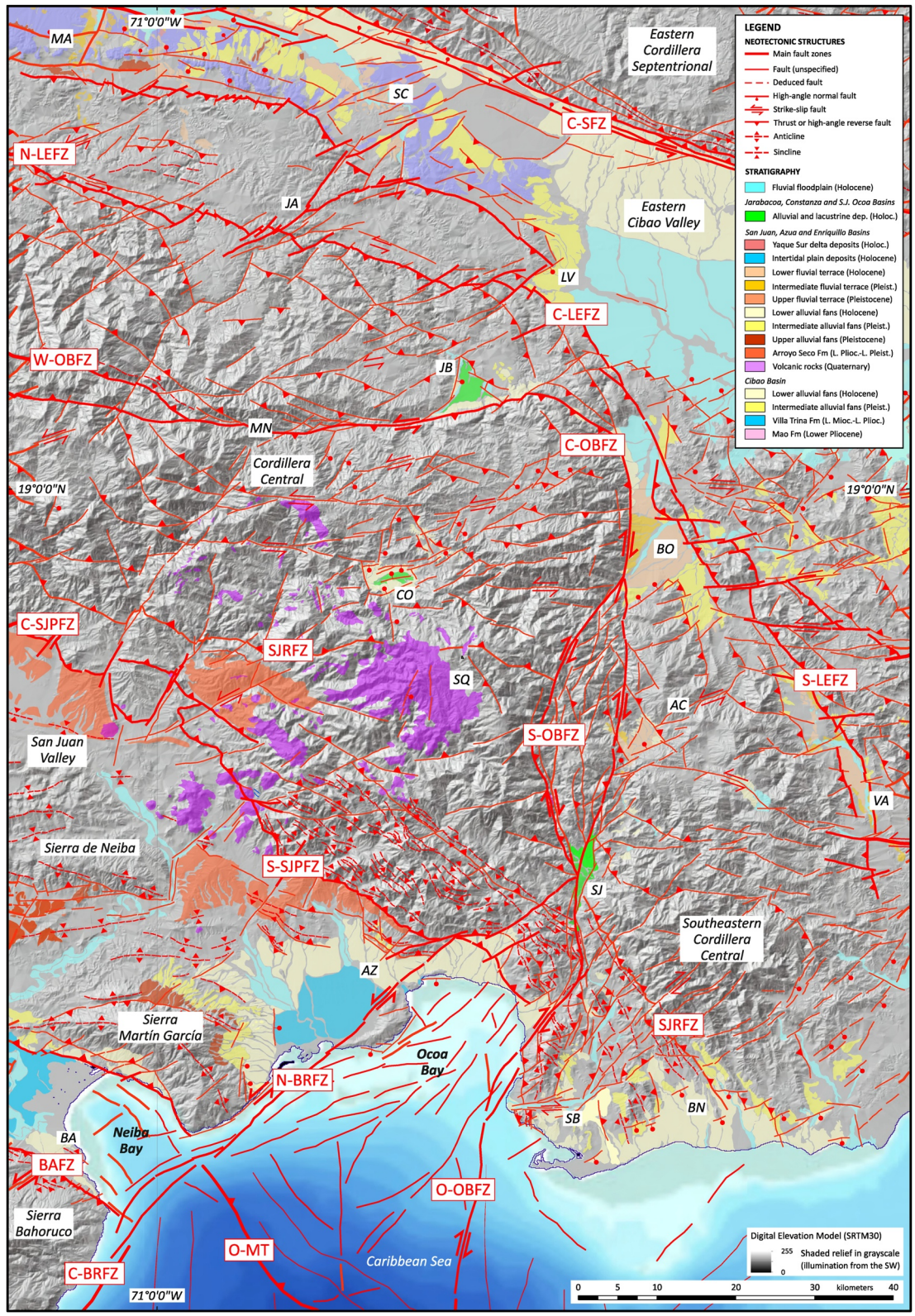

Figure 3.

The western part of the Hispaniola block comprises from N to S the Cordillera Central, the Peralta Belt, the Neogene basins of San Juan, Azua and Enriquillo, and the Muertos deformed belt, as well as the Quaternary intramountain basins of San José de Ocoa, Constanza, Jarabacoa and Bonao (Figure 2). The Cordillera Central in the Dominican Republic and its prolongation in the Massif du Nord in Haiti is a basement composed of units of oceanic provenance of Upper Jurassic-Upper Cretaceous age, structurally limited to the N by the Hispaniola fault zone (HZF) and to the S by the San José-Restauración fault zone (SJRFZ). The basement comprises fragments of Pacific-derived lithosphere, oceanic plateaus such as the Duarte Complex; basaltic units related to a mantle-plume magmatism, and igneous sequences related to subduction (Draper et al., 1994; Lewis & Draper, 1990). A regional left-lateral transpressive regime deformed the Cordillera Central basement during the Coniacian-Santonian (90–84 Ma), which was accompanied by the intrusion of gabbro-tonalitic batholiths (90–74 Ma; Escuder-Viruete et al., 2006).

The Peralta Belt (PB) is a 320 km-long and NW-trending fold-and-thrust belt formed by a thick sequence of sedimentary rocks from the latest Cretaceous to the early Miocene (Dolan et al., 1991; Hernaiz Huerta & Pérez-Estaún, 2002; Witschard & Dolan, 1990). It is separated by the NE-dipping San José-Restauración fault zone from the Cordillera Central to the N and by the NE-dipping San Juan-Los Pozos fault zone from the San Juan and Azua sedimentary basins to the S (Mann, Draper, & Lewis, 1991). The Peralta Belt evolved from a back-arc basin for the Caribbean island-arc, with deposition of Campanian to Eocene turbidites (Trois Rivières and Las Palmas Formations), to a transpressive fold-and-thrust belt during the late Eocene to early Miocene (Dolan et al., 1991; Hernáiz-Huerta, Díaz De Neira, García Senz, Deschamps, Genna, et al., 2007; Mercier de Lépinay, 1987; Witschard & Dolan, 1990). In the SE sector, the lithostratigraphic units of the Peralta Belt have been grouped into three sedimentary groups, separated from each other by major unconformities: the Paleocene-Eocene Peralta Group; the middle Eocene-early Miocene Río Ocoa Group; and the middle Miocene-Pleistocene Ingenio Caei Group (Díaz de Neira & Solé Pont, 2002; Dolan et al., 1991; Hernáiz-Huerta, Díaz De Neira, García Senz, Deschamps, Lopera, et al., 2007; Heubeck et al., 1991; Pérez-Valera, 2010). The Ingenio Caei Group unconformably overlies the Río Ocoa Group at the SE end of the Peralta Belt.

Oblique convergence and collision between the Caribbean and North American plates have produced the NW to WNW-trending San Juan, Azua and Enriquillo Neogene sedimentary basins in southern central Hispaniola (Figure 2). These basins form the southeastern extension of the Plateau Central and Cul-de-Sac basins in Haiti. Mann, McLaughlin, and Cooper (1991) and Mann et al. (1995) characterized the San Juan-Azua and Enriquillo basins as ramp basins, in which mountain blocks overthrust upward along both sides of the basin floor. Subsequent studies defined these basins as foreland flexural basins limited to the NE by SW-verging thrust systems, although the Enriquillo basin is also limited by opposite-vergence thrusts directed to the NE (Deschamps, 2004; Díaz de Neira, 2004a, 2004b; García-Senz, 2004; Genna, 2004; Hernaiz Huerta, 2004; Hernáiz-Huerta & Pérez-Estaún, 2002; Nicol, 2004). Miocene to Pliocene marine sediments filled these basins, and the resulting deposits form a 4 km-thick upward shallowing and coarsening mega-sequence (Deschamps, 2004; Díaz de Neira and Solé Pont (2002); Díaz de Neira & Solé Pont, 2002; García Senz, 2004; Genna, 2004; Hernaiz Huerta, 2004; McLaughlin et al., 1991; Nicol, 2004). In the Azua basin, the mega-sequence culminates with the continental coarse-grained clastic sediments of the late Pliocene-Early Pleistocene Arroyo Seco Formation (Fm). In the Enriquillo basin, the reef limestones and supralittoral marls of the Jimaní Fm pass upwards in the section to Early-Middle Pleistocene alluvial-fan breccias and conglomerates.

The Muertos Trough (MT) marks the trace of a ~650 km-long thrust bounding a deformed belt south of eastern Hispaniola and Puerto Rico (Figure 1). Seismic reflection profiles across the MT show an N-dipping low-angle thrust structure to a depth of 7 km, with folded sediments on top that form an accretionary prism (Dillon et al., 1996; Dolan et al., 1998; Dolan et al., 1998, 1998; Driscroll & Diebold, 1998). Therefore, the MT marks the boundary between the overlying fold-and-thrust belt and the subducting floor of the Caribbean plate. The age of initial convergence across the Muertos Trough is unknown, although it probably coincides with the end of the arc-continent collision and the onset of back-thrusting (Kroehler et al., 2011).

Figure 3. Neotectonic map of southern central Hispaniola. Shaded relief in grayscale has been made from the GMRT synthesis data set (Ryan et al., 2009) with GeoMapApp (www.geomapapp.org). Late Neogene and Quaternary lithostratigraphic units defined in the SYSMIN Project (Pérez-Estaún et al., 2007) are included in the map. Main neotectonic structures are: Offshore (O-OBFZ), Southern (S-OBFZ), Central (C-OBFZ) and Western (W-OBFZ) segments of the Ocoa-Bonao-La Guacara fault zone; Northern (N-LEFZ), Central (C-LEFZ) and southern (S-LEFZ) segments of La Española fault zone; Central (C-SFZ) segment of the Septentrional fault zone; Central (C-SJPFZ) and Southern (S-SJPFZ) segments of San Juan-Los Pozos fault zone; and Northern (N-BRFZ) and Central (C-BRFZ) segments of the Beata Ridge fault Zone. Other important onshore structures are Bahoruco fault zone (BAFZ) and Ocoa segment of the Muertos Trust (O-MT). Rest of acronyms as in Figure 1. Main locations are: AC; Arroyo Caña; AZ, Azua; BO, Bonao; BA, Barahona; BN, Baní; CO, Constanza; MA, Mao; MN, Manabao; MO, Moca; SB; Sabana Buey; SC, Santiago de los Caballeros; SJ; San José de ocoa; SQ, Sabana Quéliz; and VA, Villa Altagracia.

Located in the Gonâve microplate, the Haitian deformed belt (HDB) developed in western Hispaniola from the early Miocene onwards (Figure 1). It is bounded by the NE-dipping San Juan-Los Pozos fault zone to the N and by the Sierra de Neiba-Matheux thrust to the S. The HDB consists of a NW-trending and SW-verging sequence of stacked thrust sheets (Mann et al., 1995; Pubellier et al., 2000). The thrust bounding the NE thrust sheet of Montagnes Noires-Sierra de Neiba was activated during the early-middle Miocene and the thrust bounding the SW thrust sheet of Chaîne des Matheux-southern Sierra de Neiba developed in the middle-late Miocene (Hernáiz-Huerta, Díaz De Neira, García Senz, Deschamps, Lopera, et al., 2007; Hernáiz-Huerta & Pérez-Estaún, 2002; Pubellier et al., 2000).

Located in the Caribbean plate, the Sierra de Bahoruco belongs to the Hotte-Selle-Bahoruco terrain of the Southern Peninsula of Hispaniola (Mann, Draper, & Lewis, 1991). Its basement is constituted by the Cretaceous Dumisseau Fm that forms a 1.5 km-thick sequence of submarine basaltic flows, pyroclastic deposits and intercalations of pelagic limestones, radiolarites and siliceous siltstones, intruded by doleritic dikes and sills (Sen et al., 1988). The geochemical and isotopic characteristics of the basalts of the Sierra de Bahoruco establish a mantle-plume source, being similar to those of the volcanic rocks forming the CLIP (Escuder-Viruete, Joubert, et al., 2016; Escuder-Viruete, Súarez, et al., 2016). This basaltic basement is unconformably overlain by a 1.5 km-thick sequence of Eocene-Oligocene pelagic limestones and Miocene shallow-water marine limestones. A system of high-angle thrusts, of NW-SE trend and NE vergence, form the tectonic contact between the Sierra de Bahoruco and the Enriquillo basin (Díaz de Neira, 2004a; Hernáiz-Huerta, Díaz De Neira, García Senz, Deschamps, Genna, et al., 2007).

2.4. Cenozoic Tectonic Evolution of Southern Central Hispaniola

The Cenozoic tectonic evolution of southern Hispaniola comprises three deformational events. The first event produced stratal disruption, folding, thrusting and imbrication of the Peralta Group rocks during the late Eocene, as well as the syntectonic deposition of the Río Ocoa Group in an overlying sedimentary basin. Witschard & Dolan (1990), Dolan et al. (1991) and Heubeck and Mann (1991) propose a late Eocene SW-directed deformation of the Peralta Group in an accretionary prism setting adjacent to the SW edge of the Cordillera Central. The accretionary prism constituted the basement of the Río Ocoa Group. For these authors, the deformation was related to NE-directed subduction/underthrusting of the oceanic crust of the Caribbean plate under the Caribbean island-arc crust of the Cordillera Central. Oblique subduction of the North American continental margin beneath the NE-facing forearc of the Caribbean island-arc in northern Hispaniola, could cause the blocking of the collision zone during the middle to late Eocene and the transfer of contractive deformation to the back-arc region, generating folds and back-thrusts in the rocks of the Peralta Group (Dolan et al., 1991; Mann, Draper, & Lewis, 1991; Mann, McLaughlin, and Cooper, 1991; Witschard & Dolan, 1990). As syntectonic clastic sedimentation occurred in the overlying basin of the Río Ocoa Group until the Oligocene-early Miocene (Hernaiz Huerta & Pérez-Estaún, 2002; Heubeck & Mann, 1991), oblique northeastward underthrusting continued beneath the Peralta accretionary prism up to this time.

The second deformational event occurred in the early Miocene and consisted of folding and thrusting of the Río Ocoa Group rocks. Deformation in the Río Ocoa Group developed an SW-directed fold-and-thrust belt above a basal detachment horizon following a forward propagating sequence (Hernaiz Huerta & Pérez-Estaún, 2002; Heubeck & Mann, 1991). Thrusting continued until late Pliocene-Early Pleistocene times, as indicated by the age of the younger rocks of the San Juan-Azua basin (Arroyo Seco Fm) deformed in the footwall of the Peralta Belt frontal thrust (Díaz de Neira & Solé Pont, 2002). A similar structural relationship has been described in the Haitian deformed belt, where SW-directed thrusts affect the Miocene sedimentary rocks of the Plateau Central (Pubellier et al., 2000). This folding and thrusting event has been related to the collision between CLIP-related units of the Southern Hispaniola Peninsula and the island-arc crust of the Cordillera Central (Heubeck & Mann, 1991; Mann, McLaughlin, and Cooper, 1991).

The third deformational event extends from the late Pliocene(?) to the present-day. It consists of NE-striking right-lateral strike-slip faults that cut rocks of Peralta and Río Ocoa Groups east of the Ocoa Bay and left-lateral strike-slip faults that displace beds of early Pliocene age in the Azua basin. This event has been related to the indentation of the southern margin of Hispaniola by northeastward displacement of the Beata Ridge (Hernaiz Huerta & Pérez-Estaún, 2002; Heubeck & Mann, 1991; Mann, McLaughlin, and Cooper, 1991). The abrupt change in the regional strike of the NW-striking folds and faults of the Peralta Group to a more N-S trend in the Bahía de Ocoa is also consistent with the indenter (Pérez-Valera, 2010). The offshore bathymetric and seismic reflection data indicate that these folds and thrusts turn progressively southward to the W-E direction of the Muertos Deformed Belt (Granja Bruña et al., 2009, 2014).

3. Neotectonic Deformation Pattern of the Ocoa-Bonao-La Guacara Fault Zone

3.1. Fault Segmentation Geometry

We define the geometry and kinematics of the Ocoa-Bonao-La Guacara fault zone using structural data at macroscopic and mesoscopic scales, as well as geomorphological observations. The neotectonic map of the Ocoa-Bonao-La Guacara fault zone and surrounding areas results from the integration of new field data with the geologic map obtained by the SYSMIN Project in the Dominican Republic (Pérez-Estaún et al., 2007). The map covered the eastern Cordillera Central, the Sierra de Martín García, the eastern Cibao basin, the southeastern part of the San Juan basin and the whole Azua basin including the Baní area (Figure 3). The folds and faults of this area define three main trends: NW to WNW-trending structures, N to NE-striking faults and ENE to E-striking faults. The NW to WNW-trending D1 structures correspond to those tectonic features parallel to the main structural grain of the Cordillera Central, for example, the WNW-striking thrusts of the Peralta fold-and-thrust belt. The N-S to NE-SW D2 transverse faults are related to the Ocoa-Bonao-La Guacara fault zone itself and represent individual structural elements of the fault deformation zone, located in the central-eastern part of the study area. The ENE to E-striking faults are also transverse D2 structures concentrated in the northern sector of the studied area, close to the Cibao basin and the Septentrional fault zone.

The Ocoa-Bonao-La Guacara fault zone runs along an N to NE-striking band, 2–12 km wide and 120 km long, spreading northward from the western termination of the Muertos Trough to the Cibao basin. In the northern portion, the fault trace bends to a W-E trend over a distance of ∼30 km (Figure 3). The curved trace of the Ocoa-Bonao-La Guacara fault zone, together with changes in its kinematics (see below), enables establishing four major fault segments. From S to N, they are Offshore (O-OBFZ), Southern (S-OBFZ), Central (C-OBFZ) and Western (W-OBFZ) segments (Figure 3).

The O-OBFZ segment is about 50 km-long and runs NNE-SSW to NE-SW along the eastern margin of Ocoa Bay. It consists of a continuous NNE to NE-striking right-lateral strike-slip fault that produces a clockwise rotation and deforms the folded sediments of the Muertos accretionary prim, The O-OBFZ also bends the fold and thrust structures of the Peralta Belt, the SJPFZ and the early Miocene to Early Pleistocene sedimentary fill of the Azua basin (Figure 3). Northward, the segment overthrusts the Peralta Group rocks over Late Pleistocene to Holocene alluvial fan sediments.

The S-OBFZ segment is a roughly 50 km-long, N-striking right-lateral strike-slip fault system, that cuts at a high-angle and displaces the NW-SE structure of the Peralta Belt and the late Cretaceous volcano-plutonic basement of the Cordillera Central (Figure 3). South of San José de Ocoa, the fault trace splits into two distinct segments that converge 35 km northward into the C-OBFZ segment. Located at its southern end, the San José de Ocoa sedimentary basin formation is related to a right-hand releasing-bend between these two branches of the S-OBFZ.

The C-OBFZ segment consists of an arcuate fault about 70 km in length. In the southern part, the segment is a N to NNW-striking and W-dipping oblique right-lateral thrust that allows the late Cretaceous volcanic rocks of the Cordillera Central to overthrust the Quaternary alluvial fan sediments of the Bonao basin (Figure 3). Steep, fresh-looking scarps with triangular facets mark the E-facing frontal fault. In the northern part, the C-OBFZ segment rotates counterclockwise to a W-E to WSW-ENE trend, changing its kinematics from near pure reverse to an oblique reverse left-lateral fault. The segment separates late Cretaceous basalts from Quaternary alluvial-fluvial sediments of the Jarabacoa sedimentary basin. The fault surface has a medium dip-angle to the S and overthrusts the basalts over the gravels and sands.

The W-OBFZ segment exhibits a continuous double trace for more than 90 km, which limits an intermediate straight and narrow ridge (Figure 3). Both traces exhibit steep, fresh-looking scarps at the foot of reliefs and separate a 3 km-wide undeformed zone of the late Cretaceous Guacara tonalitic batholith. The linearity of both fault segments suggests that they are nearly vertical (i.e., N and S-dipping high-angle faults, respectively) and accommodate a predominantly left-lateral strike-slip displacement.

3.2. Regional Magnetic Data

An integration of geological-structural and magnetic data is performed to identify better the crustal blocks and their tectonic limits in southern central Hispaniola. The geophysical data comes from the magnetic and radiometric flight carried out in the context of the EU SYSMIN Project in the Dominican Republic. The methodology

10.1029/2022TC007618

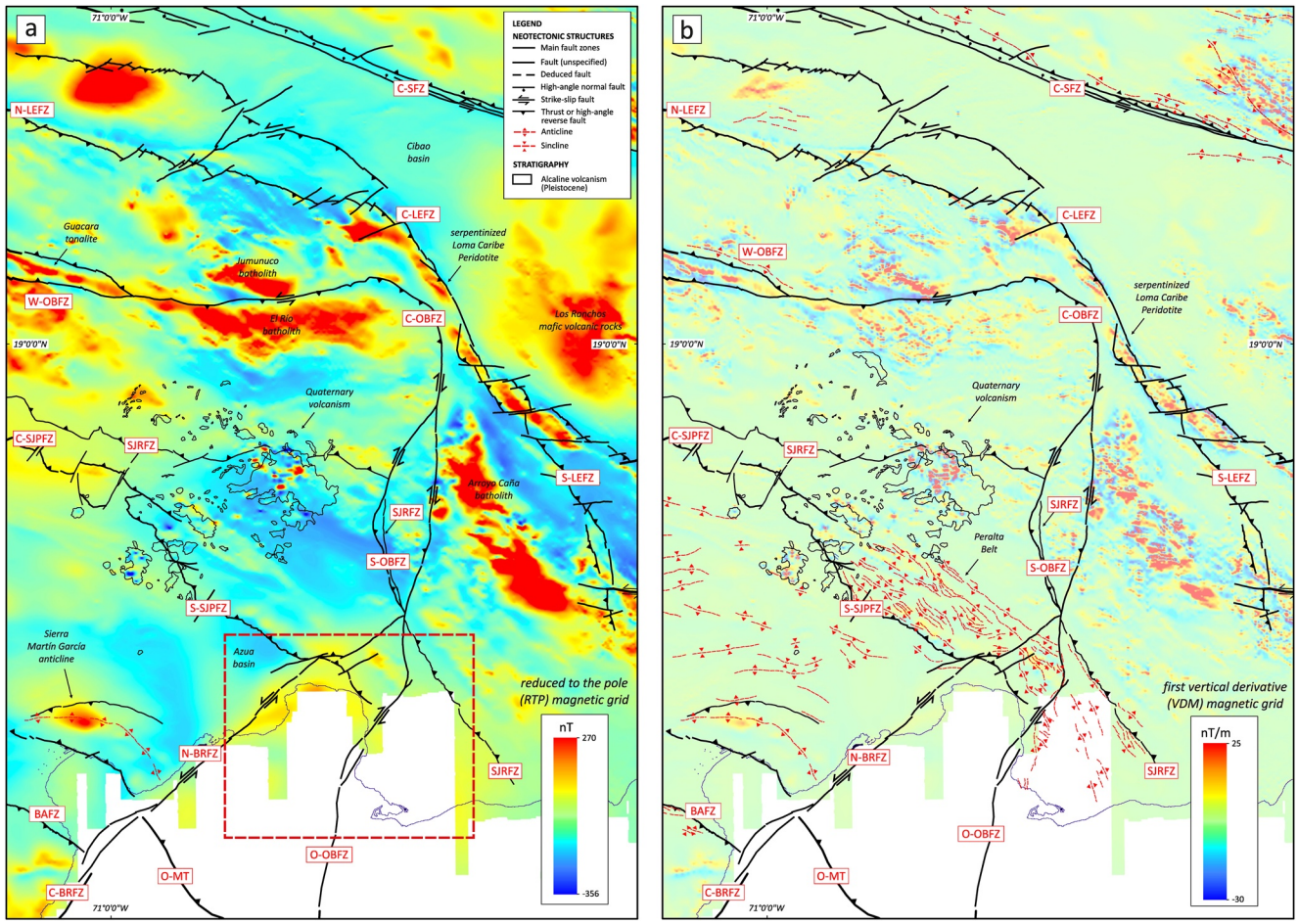

Figure 4. Magnetic maps showing major neotectonic features in southern central Hispaniola. (a) Reduced to the pole (RTP) of the total magnetic field operation improves the spatial position of anomalies that help to define areas with long and short wavelengths and tectonic boundaries between magnetic provinces. (b) The first vertical derivative operation (VDO) from the total field allows identifying trends possibly associated with tectonic boundaries and intra-basement features. Acronyms as in Figure 1. The box with the discontinuous red line marks the situation illustrated in Figure 6. See explanation in text.

of acquisition and analysis of the potential field data is explained in García Lobón and Rey Moral (2004), García-Lobón and Ayala (2007) and Ayala et al. (2017), as well as in the Supporting Information S1. Because the total magnetic intensity map responds to the sum of magnetic fields contributed by different crustal lithological units and structures, it is not possible to quantitatively classify the anomalies of the studied area using the total magnetic field. For this reason, the interpretation of the total magnetic field regional map is based in this work on its textural patterns.

The orientation of the regional magnetic field showing NW to WNW-trending subparallel bands draw the large-scale structure of southern central Hispaniola (Ayala et al., 2017). In detail, the eastern Cordillera Central and surrounding areas can be subdivided into major textural patterns in the reduced to the pole (RTP) and first-vertical-derivative magnetic grids (VDM; Figure 4). Short-wavelength magnetic signatures correspond generally to areas where the magnetic sources in the basement are located close to the surface. In the RTP magnetic grid, these areas have elongated shapes following a sub-parallel trend associated with the NW to WNW-striking regional structure of late Cretaceous amphibolites, ridges of basaltic volcanic rocks and gabbro-tonalitic batholiths of the Cordillera Central. Located in the NE boundary of this domain, the Loma Caribe Peridotite defines a strong (from 50 to 270 nT) and continuous positive magnetic anomaly, which follows a NW-SE trend for more than 80 km. The anomaly is related to titanomagnetite growth during serpentinization by tectonic exhumation and surficial alteration of the peridotites in the late Cenozoic. In turn, the southern sector of the Cordillera Central displays scattered short-wavelength anomalies, roughly elongated along a NE-SW trend, related to dyke intrusion and the emission of mafic to intermediate volcanic rocks during the Quaternary.

Areas with signatures of long-magnetic wavelengths correspond to regions where the magnetic source is located farther from the surface, or where the magnetic rock intensity in the basement is weak. The Cibao, San Juan and Azua sedimentary basins generally display long-wavelength anomalies in both the RTP and VDM magnetic grids (Figure 4). This is related to the 1 to 5 km-thick overburden of paramagnetic sediments that fill these basins, which reduces the basement magnetic intensity. The sedimentary rocks that form the Peralta belt in the SW sector of the Cordillera Central also define a pattern of long-wavelength magnetic anomalies, limited by the San José-Restauración and SanJuan-Los Pozos fault zones. However, the magnetic grid shows an unusual behavior in the sedimentary carbonate massifs of northern Sierra de Bahoruco, Sierra de Martín García and coastal sectors of the Ocoa Bay (Figure 4). These areas show long-wavelengths of relatively high-magnetic intensity (between 0 and 100 nT), suggesting a magnetic source that is much deeper than the surrounding areas. A possible explanation for this unusual magnetic signature is that the basement is composed of basalts typical of the CLIP.

The VDM grid shows juxtaposed areas of long and short-wavelength magnetic anomalies controlled by the regional macrostructure (Figure 4). Low values mark the surface trace of the main fault zones, corresponding to the different segments of the SFZ, LEFZ, OBFZ and the BRFZ. The VDM grid also shows how the NW to WNW-trending D1structures of the Cordillera Central and the San José-Restauración fault zone are cut and displaced by the transverse D2 fault system of the Ocoa-Bonao-La Guacara fault zone.

3.3. Seismicity

The distribution of historical and instrumental seismicity provides additional information on the regional tectonics of southern central Hispaniola (Figure 5). Details of the earthquakes record are included in the Supporting Information S1 and Supporting Information S2. Historical seismicity records from Hispaniola only cover the past ~500 years, beginning with the Spanish colonization. These records probably have a bias toward earthquakes that have damaged significant population centers and do not include earthquakes in low population density regions. Except for the Septentrional fault zone (Prentice et al., 2003), no historical event could be securely tied to an individual fault and the location of epicenters is derived from earthquake damage reports and regional attenuation relationships between earthquake intensity, magnitude and distance (ten Brink et al., 2011; Bakun et al., 2012).

In central Hispaniola, ten Brink et al. (2011) speculated that the 1562 (*Mw* 7.0; *Mw*, moment magnitude) and 1842 (*Mw* 7.0) earthquakes ruptured the SFZ. The intensity centers for the 1562 and 1842 earthquakes are between Santiago and La Vega, and 10 km west of Santiago, respectively. However, both intensity centers remain situated in the Cibao basin, about 15 km south of the SFZ trace (Figure 5). Bakun et al. (2012) associated the 1751 event (*Mw* 7.5) with the eastern end of the EPGFZ system that would include the exposed and blind thrust faults northwest Azua (Figure 5). For these authors, an alternative source is a *Mw* 7.5 event on the Muertos deformation belt. The location and magnitude of the *Mw* 6.0 to 7.5 earthquakes in 1615, 1684, 1691 and 1911 cannot be confidently determined with the available data, since these strong earthquakes did not produce known surface ruptures.

High instrumental seismicity is recorded along the contact between the Central and Septentrional mountain belts and the topographic depressions of the Cibao and San Juan-Azua basins. Earthquakes are shallow and usualy located at depths less than 20 km. The respective epicenters are often concentrated in, or close to, the trace of the OBFZ, C-SFZ and S-JPFZ segments (Figure 5). In particular, S and C-OBFZ segments separate an eastern area of higher earthquake density from a western area of lower density. In the eastern zone, a southern cluster of shallow earthquakes (depth < 40 km) is distinguished from a northern cluster of intermediate earthquakes ($100 <$ depth < 250 km). This distribution of seismicity delineates most of the active deforming zones. It is also consistent with the location of young tectonic landforms, fault scarps and a variety of geomorphological markers indicative of active faulting and tectonic uplift along these zones (see below).

Relatively few earthquakes with well-constrained focal mechanism, depth and location are available for southern central Hispaniola (see Supporting Information S2), which come from the Global Centroid-Moment-Tensor (CMT) catalog (Ekström et al., 2012). These moment tensor solutions indicate both thrust and strike-slip faulting. Epicenters of the 1992, 2015, and 2017 earthquakes are located close to the Ocoa-Bonao-La Guácara, San Juan-Los Pozos and San José-Restauración fault traces (Figure 5). Their focal mechanisms indicate nearly pure thrusting on WNW to NW-striking nodal planes, at depths between 15 and 23 km, and probably correspond to active mid-crustal thrusting in the Peralta and the Muertos fold-and-thrust belts.

Epicenters of the 1977 and 1988 events are also located very close to the Ocoa-Bonao-La Guácara fault trace (Figure 5). The focal mechanism of the 1988 earthquake indicates oblique reverse left-lateral strike-slip faulting

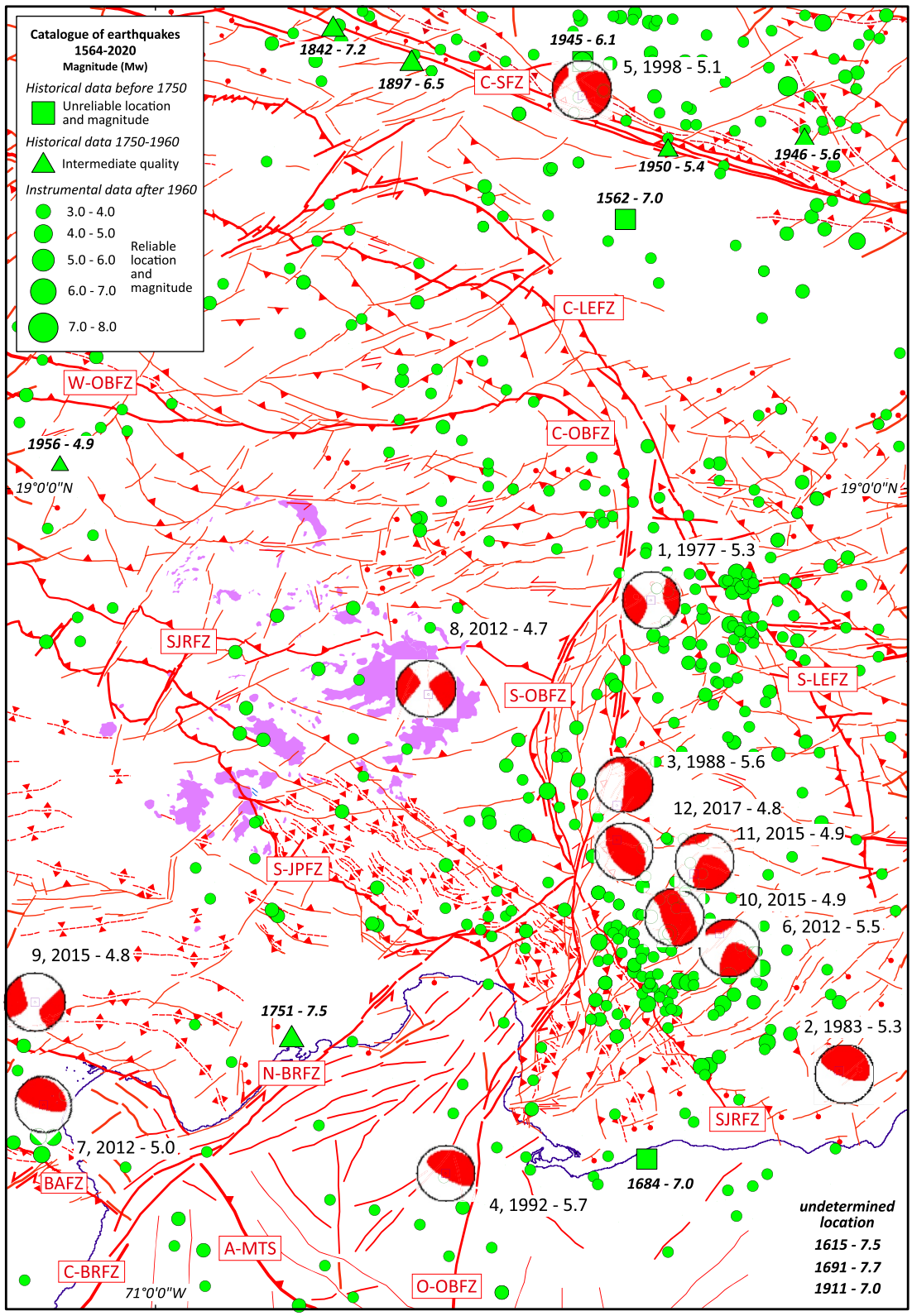

Figure 5.

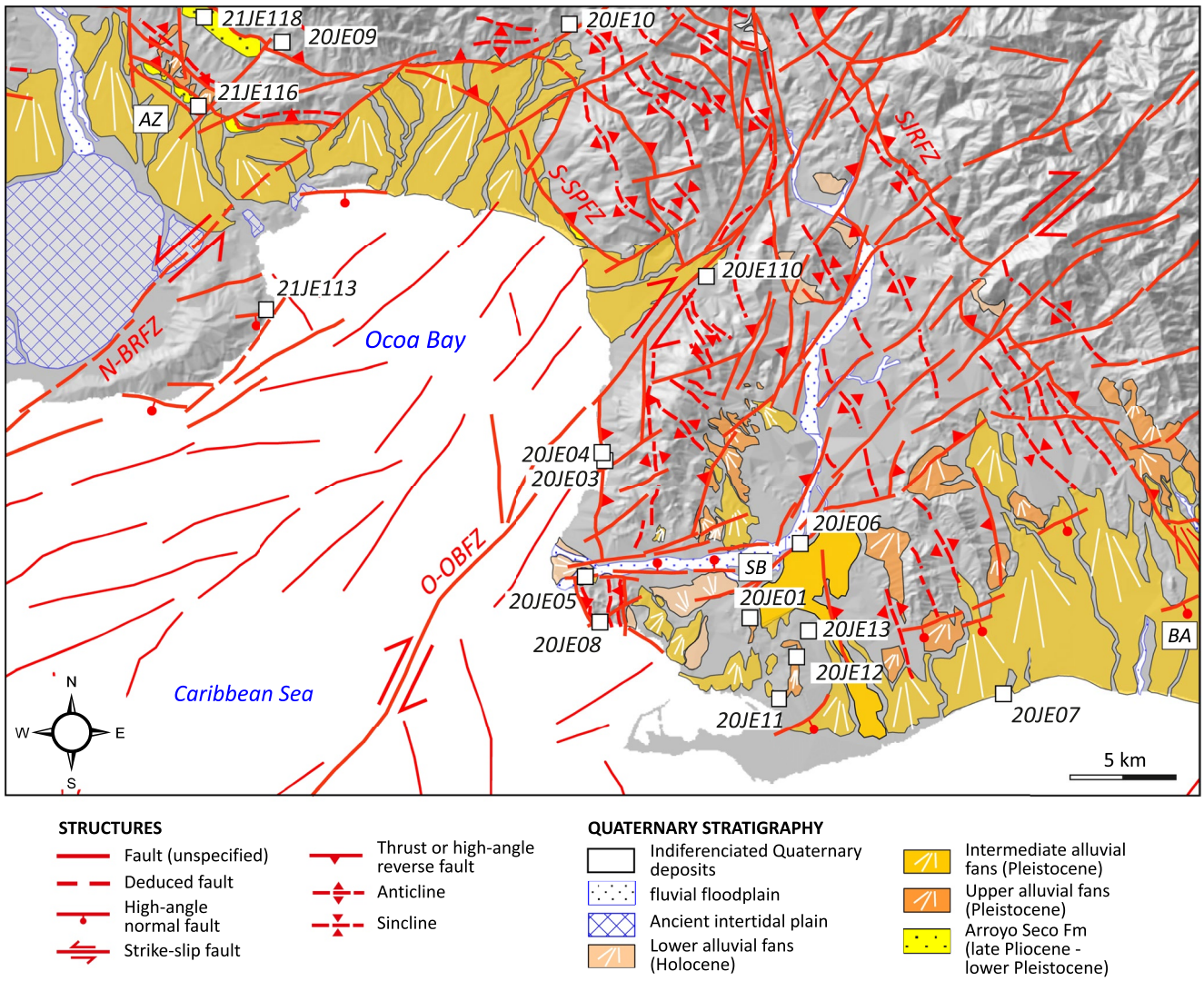

Figure 6. Structural map of the Ocoa Bay in southern Hispaniola (see location in Figure 4), showing the main Quaternary lithostratigraphic units, neotectonic structures, and sites of OSL sampling and fault-slip data measurements. Main neotectonic structures are: Offshore (O-OBFZ) segment of the Ocoa-Bonao-La Guacara fault zone; Southern (S-JPFZ) segment of San Juan-Los Pozos fault zone; and Northern (N-BRFZ) segment of the Beata Ridge fault Zone. AZ, Azua; BN, Baní; SB; Sabana Buey pull-apart basin. Rest of acronyms as in Figure 1.

on a sub-vertical NNE-SSW nodal plane, compatible with the geometry and kinematics of the S-OBFZ segment. The focal mechanism of the 1977 earthquake indicates right-lateral strike-slip faulting on a nearly vertical NNE-striking nodal plane, or left-lateral faulting along an NW-striking nodal plane, both inconsistent with the local geometry of the C-OBFZ. However, the earthquake depth is 70 km and, as the cluster of nearby intermediate earthquakes, must account for mantle level deformation. The focal mechanism solutions of 2012 and 2015 earthquakes show predominant left-lateral strike-slip faulting on NNE-trending nodal planes. These earthquakes and the nearby shallow earthquakes likely record deformation along strike-slip faults transverse to the Peralta Belt and connected with the O-OBFZ segment. The 2012 and 2015 earthquakes occurred at shallow depths (12

Figure 5. Catalog of earthquakes and focal mechanisms compiled for southern central Hispaniola. White symbols are historical and instrumental earthquakes of $Mw > 3.0$ from 1564 to 2020 A.D. Due to the high uncertainty related to the magnitude and location of historical earthquakes, they are classified into three groups following Terrier-Sedan & Bertil (2021): historical data before 1750 of unreliable magnitude and location; historical data between 1750 and 1960 of intermediate quality; and instrumental data after 1960 generally of high quality. More than 12 epicenters of earthquakes of magnitude at least Mw 6.0 are located in the study area, or the immediate surroundings They include the earthquakes of 1562 (destroyed La Vega and Santiago de los Caballeros), 1615 (destroyed Santo Domingo), 1684 (affected Azua and Santo Domingo), 1691 (destroyed Azua, affected Santo Domingo), 1751 (destroyed Azua) and 1911 (affected San Juan). Well-constrained fault plane solutions from 1976 to 2021 are taken from the Global Centroid-Moment-Tensor (CMT) Catalog (Ekström et al., 2012). Outcrops of Quaternary volcanic rocks are indicated in purple. Details on the data sources can be found in the Supporting Information S1 and Supporting Information S2. Acronyms as in Figure 1.

and 21 km) and their epicenters are located along a NE-SW alignment defined by dykes, vents and emission centers of the Quaternary alkaline volcanism (Figure 5). Their focal mechanisms indicate left-lateral strike-slip faulting on a subvertical NE-SW nodal plane, which is subparallel to the transverse NE to ENE-striking faults. The epicenter of the 2012 earthquake is located in the Neiba Bay, about 10 km north of the trace of the Bahoruco fault zone (BAFZ; Figure 5). The focal mechanism solution for this crustal event represents nearly pure thrust faulting on a gently N-dipping and WNW-trending nodal plane, or on an S-dipping and W-trending nodal plane, similar to those found by Rodriguez et al. (2018) under the Sierra de Bahoruco. Both fault planes are consistent with the structural pattern and geometry of the BAFZ and the frontal thrust of the Sierra de Martín García that are probably connected at depth.

In summary, focal mechanism solutions suggest mid-crustal thrusting below the SW-verging Peralta Belt, oblique reverse to right-lateral strike-slip faulting related to the OBFZ, and left-lateral strike-slip faulting in the western sector of the study zone. Other events indicate respective thrust and strike-slip faulting in the BAFZ and C-SFZ segments.

3.4. Quaternary Deposits

We have evaluated the Ocoa-Bonao-La Guácara fault zone neotectonic activity dating Quaternary deposits. The Quaternary sedimentary record is represented by a system of alluvial fans and intramountain basin fill in southern central Hispaniola (Figures 3 and 6). The igneous basement of the Cordillera Central, the Peralta Belt, and the NE margin of the San Juan-Azua basins were thrusted, folded and uplifted during the lower Miocene to late Pliocene (Hernáiz-Huerta & Pérez-Estaún, 2002; Heubeck & Mann, 1991). Erosion of the resulting relief produced piedmont spreading deposits at the southern and southwestern slopes of the Cordillera Central since the Early Pleistocene. These deposits have been integrated into a Quaternary morphoclimatic sequence, corresponding to the successive development of three systems of alluvial fans at different topographic levels (Díaz de Neira, 2000; Pérez-Valera, 2010).

The upper alluvial fan system forms small relict plateaus inclined toward the S and SE, over the surface of the intermediate alluvial fan system (Figure 6). It is made up of about 10 m-thick poorly consolidated sandy conglomerates and coarse debris (manly cobbles and abraded boulders) of tonalites, volcaniclastic rocks, greywackes and limestones. The intermediate alluvial fan system forms a more extensive and better preserved deposit, which connects the foot of the Cordillera Central relief with the southern coast (Figure 6). It forms a 6 to 14 m-thick sequence of conglomerates frequently filling paleochannel surfaces, very poorly consolidated and rich in a sandy matrix. Conglomerates are composed of tonalite, basalt, limestone and sandstone pebbles. The current lower alluvial fan system is spatially restricted to the Sabana Buey valley and small coastal plains of southwestern Baní (Figure 6). Its incision in the intermediate alluvial fans implies a change in the geometry of the drainage network, which has been attributed to fluvial capture processes (Díaz de Neira, 2000; Pérez-Valera, 2010). These deposits are made up of a 6 to 18 m-thick section of polymictic gravels and sands, with well-rounded clasts of limestone, volcanic rocks and sandstone.

Following the terminology of Mann (2007), the San José de Ocoa sedimentary basin is an active spindle-shaped to a lazy-S-shaped pull-apart basin of Quaternary age (Figure 3). This intramountain basin is related to a right-hand releasing-bend of the S-OBFZ segment. Localized extension produced a topographic depression confined by NNW and NNE-striking right-lateral faults, filled by poorly consolidated Quaternary alluvial-fluvial sediments. These sediments form a 2 to 26 m-thick sequence of polymictic gravels, rich in a sandy matrix, with subordinate sands and muds. The size of the pebbles varies between 5 and 15 cm, with locally rounded blocks of up to 1 m in diameter.

The Bonao basin is an active transpressional intramountain basin developed marginally of the C-OBFZ segment (Figure 3). The oblique reverse right-lateral movement of this segment subsided the eastern footwall by flexural loading of the western hanging-wall, similar to foreland basins adjacent to uplifted blocks. The basin has a N-S elongated triangular shape, in which a narrow structural depression lies parallel to the western active master faults. Its fill is characterized by an asymmetry of sediment thickness and facies pattern, with western coarse-grained proximal alluvial-fans, fed by streams from the uplifted block, and eastern fine-grained distal alluvial-fans and fluvial floodplain. Proximal facies are between 20 and 40 m-thick, consisting of quartz-rich gravel, feldspathic sand and silt. Distal facies have a visible thickness between 4 and 12 m, and are made up of sand, silt and clay.

The Jarabacoa basin is another example of active transpressional intramountain basin developed in the front of the C-OBFZ segment (Figure 3). Analogously to the Bonao basin, thrusting and loading of the southern hanging-wall block caused subsidence in the northern footwall block. The basin has a triangular shape and a filling controlled by the sedimentation of two superimposed alluvial fan systems that are strongly incised at present by the drainage network of the Yaque del Norte and Camú rivers. The older alluvial fans have a high slope and are constituted of between 10 and 36 m of massive conglomerates and orange sands. The conglomerates have centimetric clasts and scattered blocks that can reach 2 m in diameter. The younger fans have a low slope and are made up of 10–20 m of orange gravel with blocks, sand, red silt and clay.

4. Fault-Slip Data Inversion

4.1. Methodology

The paleostress regime within and around the Ocoa-Bonao-La Guácara fault zone can be evaluated using inversion methods of brittle fault-slip data. These methods assume that slip on a given fault plane occurs in the direction of the maximum resolved shear stress of a regional stress tensor (Angelier, 1994; Célérier et al., 2012). It involves collecting structural data on faults, such as plane orientation, striae direction and sense of slip from kinematic indicators at the outcrop scale. Mesoscopic kinematic indicators currently used to infer the slip-sense on the fault-plane along the striae direction are the growth of fibrous crystals in steps, R and P-Riedel shears, grooves and crescent fractures, among others (e.g., Petit, 1987). To obtain from fault-slip data the principal stress axes ($\sigma_1 > \sigma_2 > \sigma_3$) and the stress ratio $R = (\sigma_2 - \sigma_3/\sigma_1 - \sigma_3)$ that best fit the reduced stress tensor at a given site, several inversion methods have been proposed (see reviews by Célérier et al., 2012; Twiss & Unruh, 1998). Using multiple methods, hence different algorithms, increases the accuracy of the results by reducing the effect of systematic errors.

In natural conditions, fault-slip data sets measured at one site can be polyphasic, including several fault subpopulations consistent with different stress tensors. The separation of subpopulations referring to each tensor was performed prior to the inversion method for stress, calculating the pressure (P or compression axis) and tension (T or tensional axis) axes for each fault-slip data. Appearance of several clusters of P or T axes in stereographic projection was interpreted as indicative of the existence of fault-slip data related to different paleostress tensors, allowing their separation in fault subpopulations. Fault crosscutting relationships, the overprinting of several striations in the same fault plane and the absolute age of the faulted rocks have also been used as criteria to date faults and thus discriminate paleostress tensors and tectonic events.

TectonicsFP v1.7.9 software of Reiter & Acs (2000) and Ortner et al. (2002) allows plotting the fault-slip data in stereographic projection, perform a statistical analysis and obtaining a fault-slip inversion result. Fault-slip data analysis and principal stress axes calculation were first performed with the kinematic right-dihedra method (RDM; Angelier, 1994), which shows the distribution of the percentage of compression or extension dihedra in stereographic projection. Inversion of fault-slip data was accomplished next with two inverse independent methods: direct inversion (DIM) and (NDA) numeric dynamic analysis. Statistically stable stress tensors were obtained from 10 to 30 fault-slip data measured in each structural station. A further explanation of the fault-slip data acquisition and analysis is included in the Supporting Information S1.

This work calculated stress tensors from a population of 438 fault-slip data, measured in 21 sites distributed within and around the Ocoa-Bonao-La Guácara fault zone. Geological characteristics of these sites are reported in Supporting Information S3. Stress inversion of the fault-slip data yields 28 stress tensors and their respective plots are shown in Figures 7–13. This compilation of stress tensors includes data derived from faults measured in late Cretaceous to Quaternary rocks. The orientation of their maximum horizontal stress, stress regime, kinematic type of faults and the immersion method used in each site, which is generally consistent with each other, are included in Supporting Information S4. Combined detailed structural analysis, fault-slip data inversion, and geochronology show that the deformation can be divided into three main events (D1-D3; see below).

4.2. Fault-Slip Data Inversion in the Peralta Belt

The site 20JE08 is located in the southernmost outcrops of the Peralta Belt, about 5 km east of the O-OBFZ segment in the eastern sector of the Ocoa Bay (Figure 6). In this sector, the structures of the Peralta Belt present a rotated N-S trend with respect to the WNW-ESE regional orientation. At this site (Figure 7), the macrostruc-

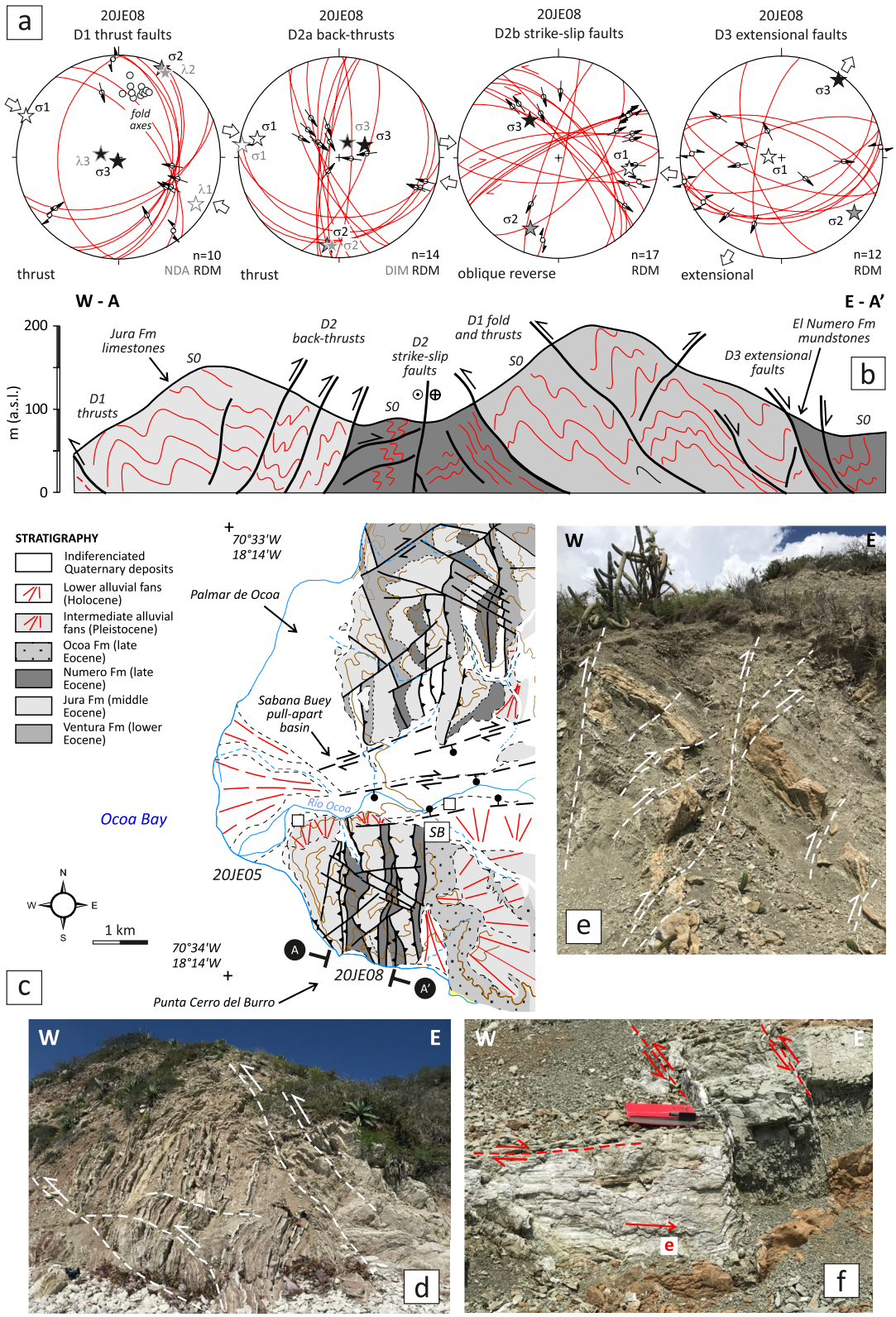

Figure 7.

ture consists of a hectometric imbrication of the middle Eocene limestones of the Jura Fm and the late Eocene thin-bedded turbidites of the Numero Fm, related to a D1 deformation in a fold-and-thrust belt of N-S trend and W-directed vergence. This macrostructure is affected by a set of N-trending and E-verging D2a back-thrusts, as well as by a system of high-dip angle (>60°) strike-slip faults D2b. The D2b fault system comprises NE to ENE-striking right-lateral strike-slip faults and NW to NNW-striking left-lateral strike-slip faults, antithetical to the previous ones. E to ENE-trending D3 normal faults locally truncate the assemblage, exhibiting a high-dip angle toward the N and S.

Fault-slip data measurements at site 20JE08 show four contrasting subpopulations (Figure 7). Both reverse dip-slip and oblique reverse left-lateral slip vectors in medium to high-dip angle fault planes represent the first population. The second population is mainly reverse, associated with dip-slip striae. Striations with a low-pitch angle in subvertical fault planes characterize the third population. The fourth population is mainly extensional, associated with normal dip-slip and oblique normal right-lateral slip vectors. These subsets represent four successive stress regimes: the first corresponds to a transpressional stress regime D1 characterized by a N295°E trending σ_1; the second adjusts to a purely compressional stress regime D2a with a N283°E trending σ_1; the third corresponds to a near strike-slip stress regime D2b with a σ_1 of similar orientation to the second stress state; and the fourth matches with an extensional regime (to transtensive) D3 with a N036°E trending σ_3 (Figure 7).

The site 21JE110 is located at the northern Sierra del Número, on the highway from Baní to Azua, approximately 500 m east of the onland trace of the O-OBFZ segment (Figure 6). At this site, the mudstone-rich siliciclastic rocks of the lower Eocene Ventura Fm exhibit 1 to 100 m-thick zones of intense stratal disruption, which were interpreted por Witschard & Dolan (1990) as thrust surfaces in the late Eocene Peralta accretionary prism. Mesoscopically, these disrupted zones are characterized by boudinaged sandstone beds in lozenged blocks, tight to isoclinal folds with rootless limbs, asymmetric S-C structures, and a pervasive scaly clay fabric (Sp) in mudstone interbeds (Figure 8). The planar fabric (Sp) often contains a SE to S-trending calcite stretching lineation (Lp) subparallel to the fold axes. All these structures are typical of a block-in-matrix fabric of a tectonic mélange, produced initially by subhorizontal layer-parallel extension and subsequently by heterogeneous shearing (e.g., Escuder-Viruete & Baumgartner, 2014; Festa et al., 2012). In contrast, the carbonate rocks of the Jura Fm are generally stratally coherent and the strain was take up by open-to-tight folds and related solution cleavage. Stratally disrupted zones in the Ventura Fm are cut by later, out-of-sequence D1 thrust surfaces that typically dip 10°–40° more deeply than the Sp fabric, when they are restored to the original horizontal position. Both the block-in-matrix fabric and the out-of-sequence thrusts are cut by D2a back-thrusts and oblique reverse faults of W-E strike and dipping a high-angle to the NW (Figure 8). All these structures are truncated by WNW to W-striking left-lateral faults D2b and by high-dip angle normal faults D3.

Fault-slip data inversion enables the separation of populations related to three distinct stress regimes (Figure 8). The first population is represented by variably oblique reverse slip vectors in high-dip angle faults. It corresponds to a transpressional stress regime D2a characterized by a N294°E trending σ_1. The second population contains oblique reverse left-lateral slip vectors in ENE to WNE-striking sub-vertical faults. They are related to a transpressional stress regime D2b characterized by a N216°E trending σ_1. The third population includes normal vectors along predominantly dip-slip striae, and corresponds to an extensional stress regime D3 with a N346°E trending σ_3.

Sites 20JE09 and 21JE116 are located near to Azua, close to the San Juan-Los Pozos fault zone (Figure 6). On both satellite images and field observations, the SJPFZ trace corresponds to a NW-striking trust that superposes mudstones with olistolites of the late Eocene Ocoa Fm over conglomerates of the late Pliocene to Early Pleistocene Arroyo Seco Fm. Toward the SE, the SPFZ trace turns progressively toward a N-S trend and it is cut and displaced by D2b strike-slip faults. Site 20JE09 is located in the hanging-wall block, about 700 m northward of the SPFZ trace, where the limestones of the lower Miocene Sobrerito Fm exhibit structures related to D1

Figure 7. Structural analysis of the Peralta Belt. (a) Stereoplots of the principal stress-axes obtained from inversion of fault-slip data. *n*, number of data. Inversion methods: PTM, P–T Method; RDM, Right Dihedra Method; DIM (Direct Inversion Method); and NDA, Numerical Dynamic Analysis Method. (b) Cross section across the Peralta Belt in Punta Cerro del Burro (20JE08). (c) Structural map of the Peralta Belt and the Quaternary Sabana Buey pull-apart basin, showing the location of the A-A' cross-section. (d) W-vergent D1 fold-and-thrust system developed in the late Eocene thin-bedded turbidites of the Numero Fm. (e) E-vergent D2a back-thrust and reverse faults. (f) System of conjugate D2b strike-slip faults. Note the low-pitch angle of the striations [e] in the fault plane. Details of the site location, geological characteristics, and results of the fault-slip data inversion are included in the electronic Supporting Information S3 and S4.

10.1029/2022TC007618

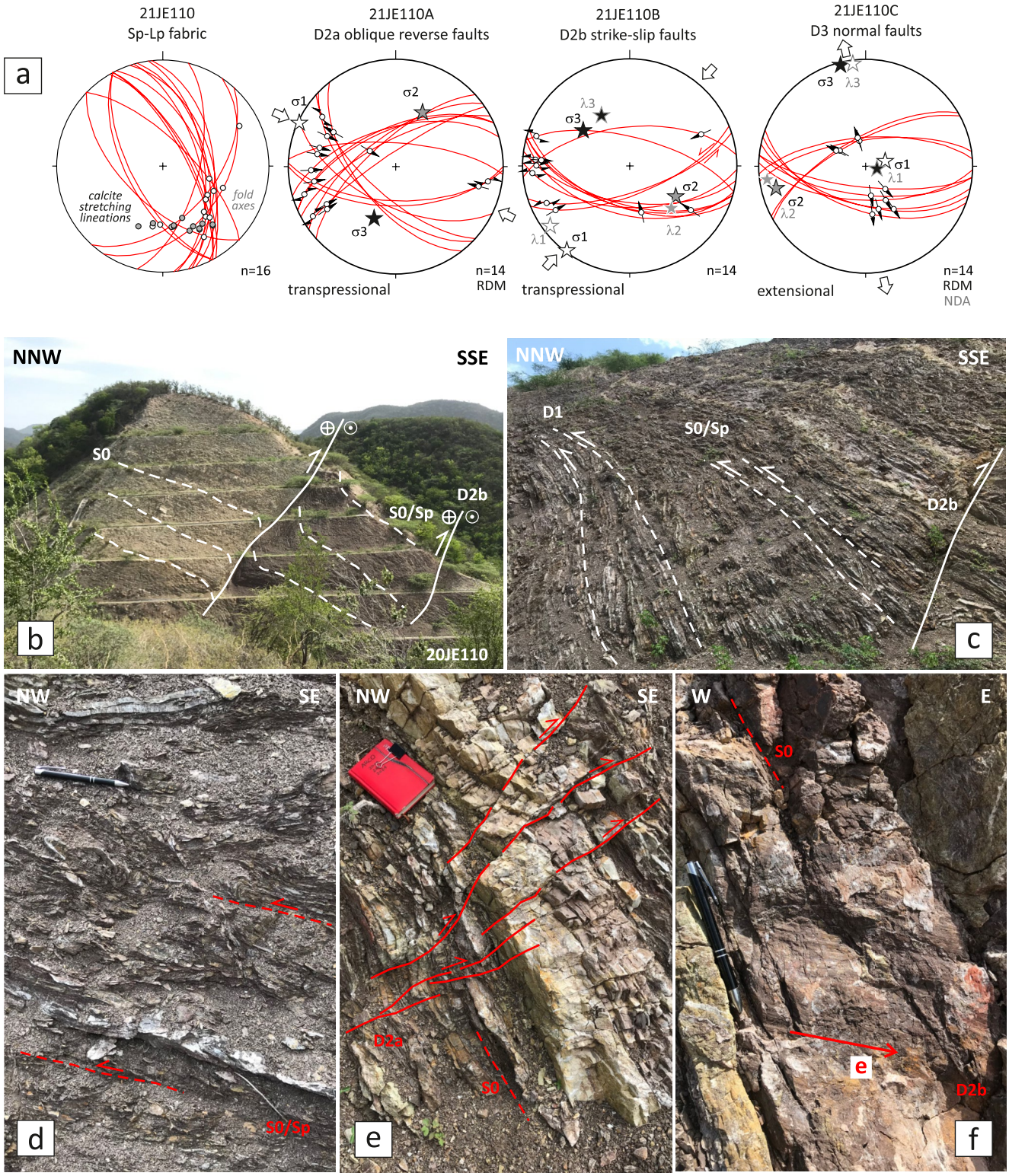

Figure 8. Structural analysis of the Peralta Belt. (a) Stereoplots of the principal stress-axes obtained from inversion of fault-slip data (see Supporting Information S3 and S4). (b) SE-vergent D2a back-thrusts and oblique reverse faults deforming the block-in-matrix fabric (Sp) in the mudstone-rich siliciclastic rocks of the lower Eocene Ventura Fm and the bedding (S0) in carbonate rocks of the Jura Fm. (c) Out-of-sequence D1 thrust surfaces cutting the block-in-matrix fabric (Sp) in the Ventura Fm. (d) Zone of stratal disruption in the Ventura Fm, characterized by boudinage of sandstone beds, tight to isoclinal folds with rootless limbs, and a pervasive scary clay fabric (Sp) in mudstone interbeds. (e) Detail of the oblique reverse faults D2a cutting the bedding (S0) in the carbonate rocks of the Jura Fm. (f) Left-lateral strike-slip fault surface D2b affecting the bedding (S0) in the Jura Fm. Note the low-pitch angle of the groove.

deformation (Figure 9). These structures consist of NW-trending and SW-verging asymmetric folds, associated with mid-dip angle faults inclined to the NE, subparallel to the SPFZ. The mesoscopic S-C structures and other kinematic indicators imprinted on the fault planes establish a top to-the-SW reverse movement. Dip-slip striae in the fault planes define a reverse faults population, which is compatible with a thrust faulting stress regime and a N346°E trending compressional axis (Figure 9).

Site 21JE116 is located in the footwall block, 4 km southwest of the SJPFZ, near the village of Azua. At this site, several NW-striking fault traces corresponds to the D1 thrust ramps associated with SW-verging anticlines. These fault-propagation folds are related to the thrust front advance in depth. In the more external anticline, conglomerates and mudstones of the Arroyo Seco Fm overthrust the gravels of the Quaternary intermediate alluvial fan (Figure 6). Slip measurements in conglomerate of the Arroyo Seco Fm, located on the subvertical southwest flank of the fold, define a population of WNW-striking oblique reverse faults and subordinated NE-striking left-lateral strike-slip faults (Figure 9). This population corresponds to a purely compressional stress regime with a N044°E trending σ_1.

Site 20JE10 is located close to the onland trace of the N-BRFZ, 15 km northeast of Azua, on the road to río Banilejo (Figure 6). Deformation related to this segment produced the clockwise rotation of the Peralta Belt fold-and-thrust belt. Late NE to ENE-striking left-lateral D2b strike-slip faults cut these D1 structures. Fault-slip measurements on mundstones of the late Eocene Ocoa Fm define two contrasting subsets (Figure 9). The first subset is reverse to oblique reverse and is associated to striations with a high-pitch angle in NW-striking fault planes. Oblique reverse slip vectors in conjugate right- and left-lateral faults represent the second subset. The first population corresponds to a compressional stress regime D1 with a N047°E trending σ_1 and the second population establishes a purely strike-slip stress regime D2b characterized by a N044°E trending σ_1 (Figure 9).

4.3. Fault-Slip Data Inversion in the O-OBFZ Segment

Sites 20JE03 and 20JE04 are located close to the onland trace of the O-OBFZ segment, 2.5 km north of Palmar de Ocoa, on the eastern sector of the Ocoa Bay (Figure 6). In the 20JE03 site, W-verging D1 folds and NE to ENE-striking strike-slip D2b faults deform the limestones and mudstones of the Jura and Numero Fms (Figure 10). These strike-slip faults also juxtapose the Peralta Belt rocks to poorly consolidated gravels and muds of the Quaternary intermediate alluvial fan. The internal structure in the alluvial fan deposit defines a syncline of NNE-SSW trend and hectometric wavelength, which appears truncated on the flanks by D2b strike-slip faults (cross section in Figure 10). The syncline gravels have provided OSL ages of 11.5 ± 0.8 ka and 12.6 ± 1.2 ka (20JE03A and 20JE03b samples), which enable to establish a Late Pleistocene age for the D2b deformation. The rocks of the Peralta Belt and the folded and faulted deposits of the alluvial fan are unconformably overlain by the subhorizontal gravels and muds of a younger alluvial fan, unaffected by either the D2b faults or the syncline structure (Figure 10).

About 500 m to the north, in the 20JE04 site, both the mudstones of the late Eocene Número Fm and the marls and conglomerates of the middle Miocene-Pliocene Arroyo Blanco Fm occur deformed by a conjugate system of NE to E-striking D2b strike-slip faults. Fault planes are generally very steep (dip > 70°) and striations indicate left- and right-lateral motions along conjugate fault planes, with a small reverse component (pitch < 20°). Fault-slip data inversion reveals a transpressional D2b stress-field ($\sigma_2 \sim \sigma_3$) with a N078°E trending σ_1 stress axis (Figure 10). The faulted assemblage appears unconformably overlain by a 3–4 m-thick fossil coral reef terrace and a 1–2 m-thick clastic unit that includes reworked coral blocks and cobbles (Figure 10). A *Diploria sp*. collected toward the base of the coral terrace has provided a U-Th age of 106.0 ± 0.54 ka (20JE04A), so its growth took place in the interglacial marine oxygen isotope stage (MIS) 5c (work in progress). The fossil wave-cut platform of the terrace is tilted 6° toward the NW. The clastic deposits of the younger (lower) alluvial fan overlie the coral reef terrace and has provided an OSL age of 5.9 ± 0.6 ka (20JE04E). Both the coral terrace and the lower alluvial fan appear deformed by a system of NE-striking normal faults filled by subvertical calcite veins, which establish an extensional stress D3 regime characterized by a NW-trending σ_3 axis.

Sites 20JE11, 20JE12, and 20JE13 are located in the wind turbine park, 4 km southeast of Sabana Buey, close to structures of the O-OBFZ (Figure 6). At these sites, the clastic deposits of the upper and intermediate alluvial fans are heterogeneously deformed by structures regionally related to this segment, as hectometric to kilometric-scale subparallel faults and the Quaternary Sabana Buey pull-apart basin. The sandy gravels of site 20JE11 are locally

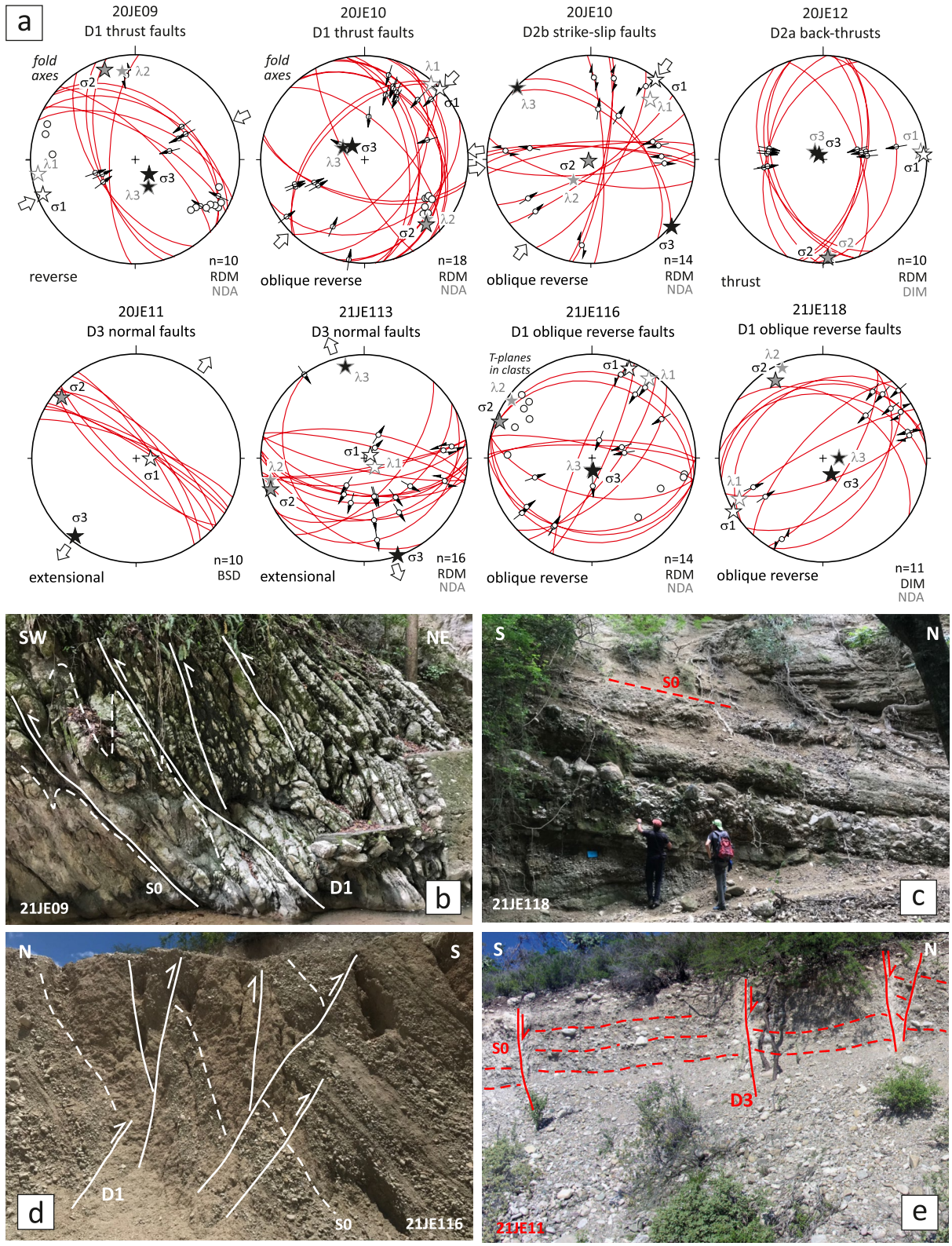

Figure 9. Structural analysis of the Peralta Belt and O-OBFZ segment. (a) Stereoplots of the principal stress-axes obtained from inversion of fault-slip data (see Supporting Information S3 and S4). (b) Asymmetric D1 folds of SW vergence, associated with mid-dip angle reverse faults, developed in the limestones of the lower Miocene Sobrerito Fm. (c) Conglomerates of the late Pliocene to Early Pleistocene Arroyo Seco Fm in the footwall block of the San Juan-Pozos fault zone. (d) Conglomerates of the Arroyo Seco Fm located on the subvertical southwest flank of a D1 anticline. Bedding (S0) is deformed by WNW-striking oblique reverse faults related to the SW-verging D1 folding. (e) Gravels rich in a sandy matrix of the upper alluvial fan deformed by D3 normal faults.

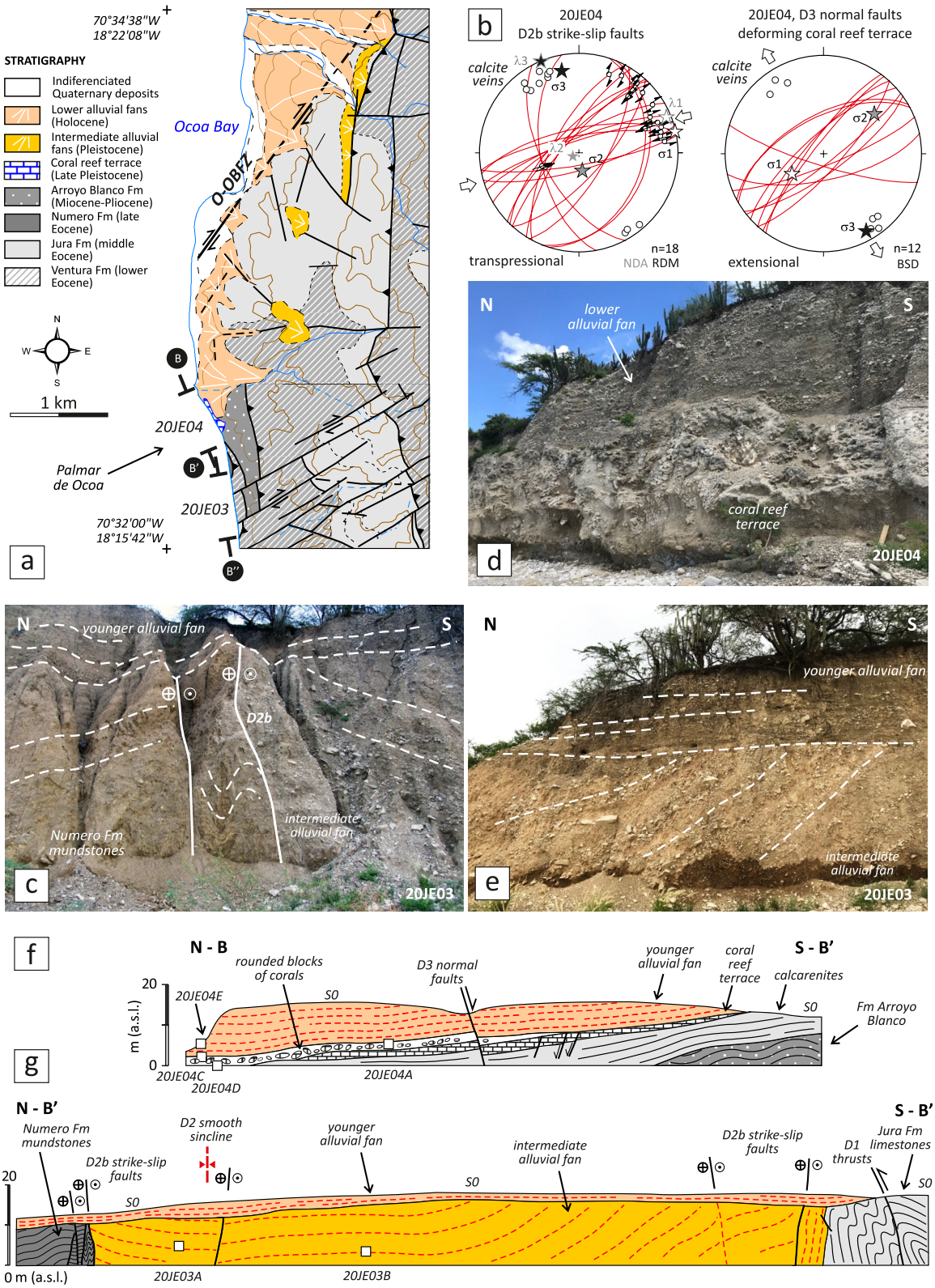

Figure 10.

deformed by a NW-striking normal fault system, produced by an extensional stress regime D3 in which σ_3 presents a N218°E orientation (Figure 9). These deposits have provided an OSL age of 13.9 ± 2.2 ka, enabling a latest Pleistocene-Holocene age to be established for the D3 deformation. The sandstones and marls of the Ocoa Fm at site 20JE12 form part of the subvertical flank of a N-trending and W-verging D1 fold, deformed by a system of high-dip angle D2a back-thrusts directed to the E. Slip measurements on NNW to NNE-striking, W-dipping fault planes affecting these rocks define a mainly reverse population, associated with dip-slip striae. This population corresponds to a purely compressional stress regime with a N087°E trending σ_1 (Figure 9). D1 and D2a Structures do not deform the gravels and muds of the upper alluvial fan, which at site 20JE13, located 1 km to the NE, have provided an OSL age of 43.8 ± 8.3 ka (Figure 6). These relationships establish a pre-Late Pleistocene age for the D1 and D2a deformations.

4.4. Fault-Slip Data Inversion in the S-OBFZ Segment

Sites 20JE15 and 21JE107 are situated in the San José de Ocoa pull-apart basin. The site 20JE15 is located just on the western edge of the basin, near the San José de Ocoa village. A west facing 40 m-high scarp marks the eastern strand of the S-OBFZ segment. This segment tectonically juxtaposes the folded and faulted rocks of the Peralta Belt to the E and the gravels and sands of the Quaternary fill of the basin to the W (Figure 11). At this site, the S-OBFZ trends NNE-SSW and has a high-dip angle to the E. Some metric-scale faults parallel to the segment cut the gravel bedding, which appears tilted about 25° to the W. Striations measured on mudstones of the Numero Fm and on pebbles from the Quaternary deposit define a population of oblique reverse right-lateral slip vectors, compatible with a D2b strike-slip regime and a N186°E trending σ_1 stress axis (Figure 11). The orientation of calcite veins and T-planes in clasts of the conglomerates establish a consistent ENE to NE trend of subhorizontal extension.

Site 21JE107 is located at the southern end of the San José de Ocoa basin, where the S-OBFZ splits into two N to NNE-striking branches that tectonically bound the basin. At this site, the S-OBFZ brings the folded limestones of the Jura Fm into tectonic contact with the subhorizontal poorly consolidated conglomerates of the basin fill. Slip measurements show two deferents populations: oblique reverse left-lateral and dip-slip reverse vectors; and strike-slip to oblique normal left-lateral vectors (Figure 11). These two populations represent two successive stress fields: the first corresponds to a transpressional D1 stress regime with a N194°E trending σ_1; and the second corresponds to a more purely strike-slip D2b regime characterized by a N187°E trending σ_1.

4.5. Fault-Slip Data Inversión in the C-OBFZ Segment

Sites 20JE16 and 20JE17 are located along the C-OBFZ segment, about 5 km SW of Bonao village (Figure 12). This fault segment exhibits a fresh N-S scarp and represents the active boundary between the 1,700 m elevated mountains of the Cordillera Central to the W and the 200 m elevated Bonao basin to the E. Along this morphological step, the fault zone produces triangular facets, perched valleys, and dextral offsets of streams that testify its recent fault activity. The C-OBFZ has controlled the sedimentation of two systems of alluvial fans and related fluvial terraces that fill the Bonao basin (Figure 12). The segment deforms the gravels and sands of the intermediate fluvial terrace of the Yuna River, which yields an OSL age of 41.2 ± 6.2 ka (20JE18), providing evidence of fault activity in the Late Pleistocene. In the site 20JE16, several metric to decametric-scale faults subparallel to the C-OBFZ segment deform the late Cretaceous volcanic rocks of the Tireo Group. Low-pitch angle striations measured on these NNE to NE-striking fault planes establish a strike-slip D2b regime characterized by a N033°E trending σ_1 (Figure 12). Site 20JE17 is located on a NNE-trending compressional ridge of hectometric-scale, bounded by two branches of the C-OBFZ segment. Reverse dip-slip striae measured in NW to N-striking fault planes affecting the volcanic rocks of the Tireo Group are compatible to a compressional regime associated with a N041°E trending σ_1 axis (Figure 12).

Figure 10. Structural analysis of O-OBFZ segment. (a) Structural map of the Palmar de Ocoa zone, showing the location of the B-B'-B'' cross-section. (b) Stereoplots of the principal stress-axes obtained from inversion of fault-slip data (see Supporting Information S3 and S4). (c) Strike-slip faults juxtaposing folded mundstones of the Numero Fm to the poorly consolidated gravels and muds of the Quaternary intermediate alluvial fan. Gravels have provided OSL ages of 11.5 ± 0.8 ka and 12.6 ± 1.2 ka (20JE03A and 20JE03b), which permit establishing a Late Pleistocene age for D2b deformation. (d) Fossil coral reef terrace of the marine oxygen isotope stage 5c overlain by gravels of the younger (lower) alluvial fan, which yields a OSL age of 5.9 ± 0.6 ka (20JE04E). (e) Folded deposits of the intermediate alluvial fan unconformably overlain by the subhorizontal gravels and muds of the younger (lower) alluvial fan. (f and g) B-B'-B'' cross-section through the Palmar de Ocoa. See text for an explanation.

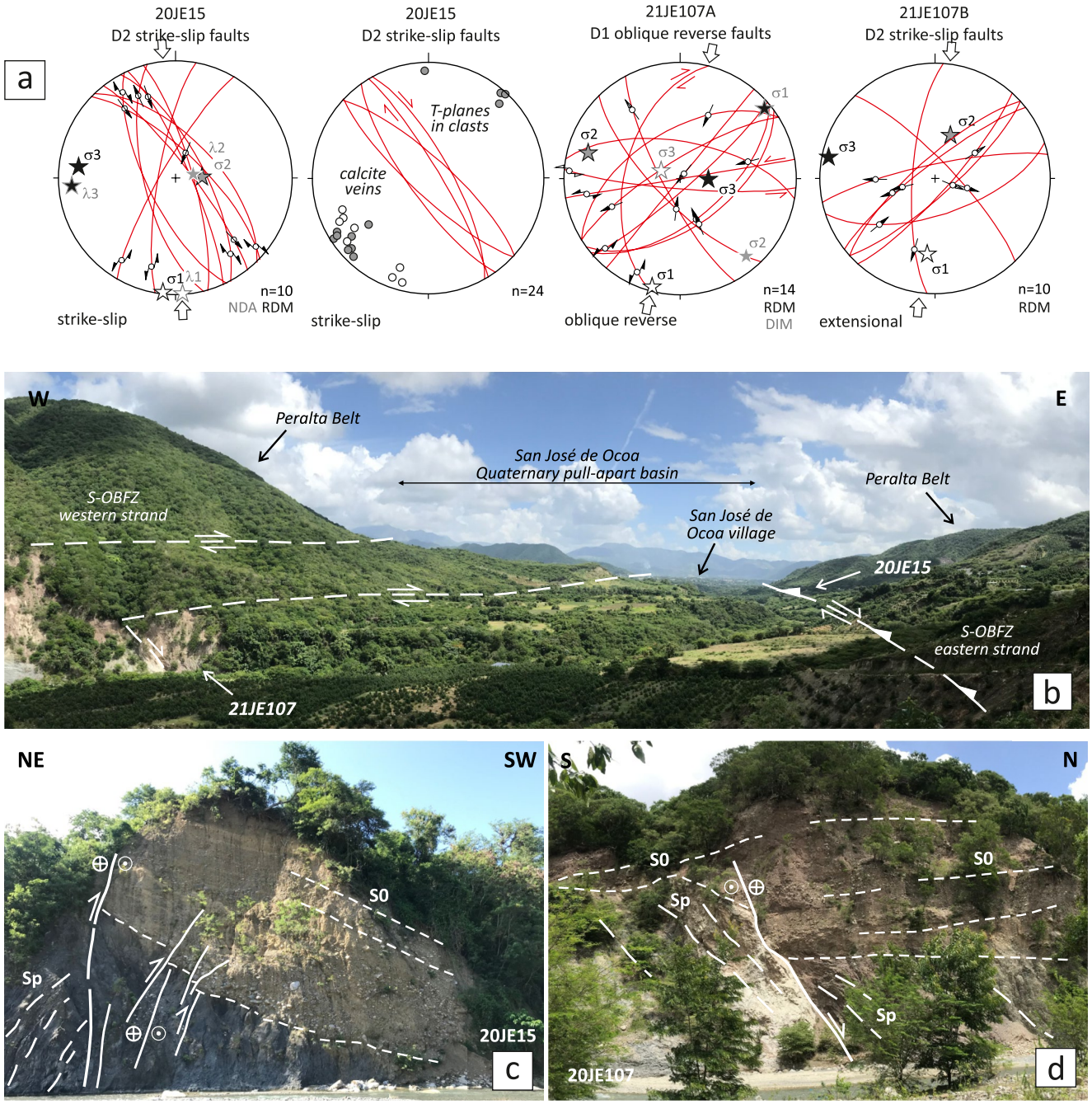

Figure 11. Structural analysis of S-OBFZ segment. (a) Stereoplots of the principal stress-axes obtained from inversion of fault-slip data (see Supporting Information S3 and S4). (b) View looking N of the Quaternary San José de Ocoa pull-apart basin, limited by the eastern and western strands of the S-OBFZ segment. (c) Tectonic contact between the folded and faulted mudstones of the Numero Fm and the gravels and sands of the basin through a subvertical fault system of oblique reverse right-lateral slip movement. Note the westward tilting of the Quaternary deposits. (d) Tectonic contact between the folded limestones of the Jura Fm with the poorly consolidated subhorizontal conglomerates of the basin.

Sites 20JE29 and 20JE66 are located along the C-OBFZ fault segment, northwest of Bonao village, on the road to Constanza (Figure 12). This segment is a NE-directed oblique thrust on the 20JE29 site that overthrusts the volcanic rocks of the Tireo Group over the gravels and sands of the Quaternary lower alluvial fan. Fault-slip measurements define a population of oblique reverse right-lateral slip vectors, associated to low-pitch striations in N-striking and W-dipping fault planes subparallel to the C-OBFZ trace. This population correspond to a compressional D2 stress regime associated with a N033°E trending σ_1 axis (Figure 12). Site 20JE66 is located in the

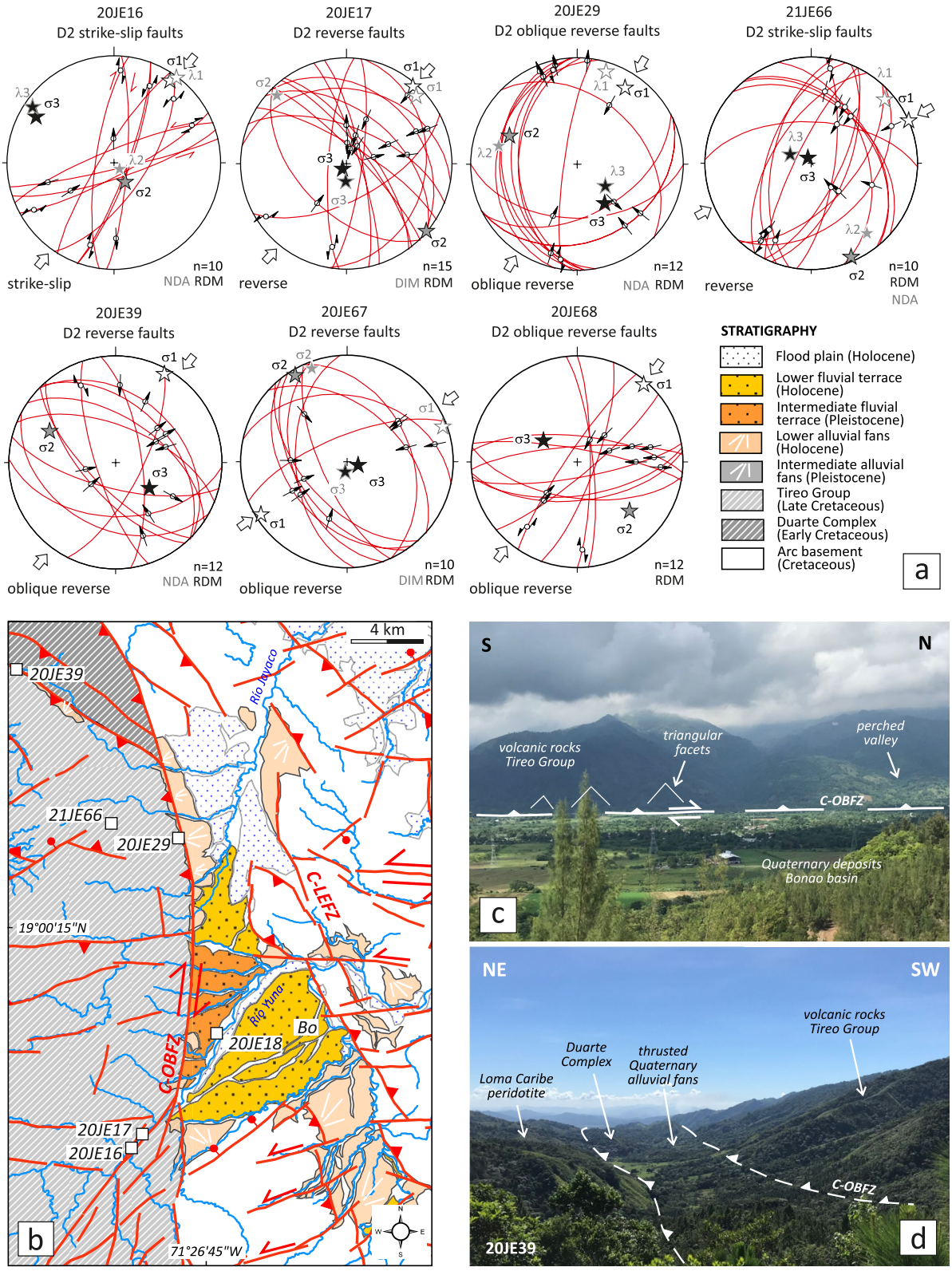

Figure 12. Structural analysis of C-OBFZ segment. (a) Stereoplots of the principal stress-axes obtained from inversion of fault-slip data (see Supporting Information S3 and S4). (b) Structural map of the C-OBFZ segment and the Quaternary Bonao basin. Bo, Bonao village. (c) View looking W of the Cordillera Central mountain front formed by the C-OBFZ near the Bonao village. Note the sharp edge to the topography, the perched valleys and the triangular facets. (d) Panoramic view of the thrust contact between the volcanic rocks of the Tireo Group in the hanging-wall block, the Quaternary alluvial fans and the metamorphic Duarte Complex in the footwall block.

hanging-wall block of the C-OBFZ, approximately 3.5 km west of site 20JE29. Two main types of metric-scale faults deform the volcanic rocks of the Tireo Group: NW-striking and NE-dipping faults with associated reverse dip-slip striae; and NNE to NE-striking and NW to SE-dipping faults, characterized by right-lateral strike-slip vectors. Both fault types collectively define a compressional D2 regime with a N067°E trending σ_1 (Figure 12).

At site 20JE39, the C-OBFZ trace is marked by a NE-facing 800 m-high morphologic scarp, which corresponds to the NW-striking frontal thrust that juxtaposes the volcanic rocks of the Tireo Group and the amphibolites and metabasalts of the Duarte Complex (Figure 12). In detail, the thrust is composed by several imbricate structures that crosscut a lower alluvial fan. Striations measured in decametric-scale fault planes subparallel to the SW-dipping surface of the C-OBFZ, as well as on other NE-dipping conjugate planes, are compatible with a transpressional D2b regime, characterized by a N029°E trending σ_1 (Figure 12).

4.6. Fault-Slip Data Inversion in the C and W-OBFZ Segments

The C-OBFZ segment represents the active tectonic boundary between a 1,500 m high mountainous zone of the Cordillera Central to the S and the 500 m high Jarabacoa sedimentary basin to the N. In parallel to a rotation of the segment trend from NW-SE to W-E and WSW-ENE, it changes its kinematics from near pure reverse to an oblique reverse left-lateral displacement. Several sites were selected along the C-OBFZ fault segment, SE of Jarabacoa village, on the road to Manabao (Figure 13). In this sector, the basalts and pyroclastic rocks of the Tireo Group overthrust the Quaternary alluvial-fluvial deposits of the Jarabacoa basin or its late Cretaceous gabbro-tonalitic basement. Preliminary radiocarbon dating of interbedded carbonaceous deposits in the sands of the lower fluvial terrace yield an age of 42,598 ± 370 cal BP (20JE54B, work in progress) that evidence a C-OBFZ activity in the Late Pleistocene.

Fault-slip vectors measured in the Tireo Group at site 20JE52 are of two main kinematic types: WNW-striking and SW-dipping faults, associated with reverse dip-slip striae; and NE to ENE-striking and SE-dipping faults, with oblique reverse left-lateral displacements (Figure 13). Inversion of the whole striae population by the RDM and DIM methods yields a compressional D2b regime characterized by a N009°E and N057°E trending σ_1, respectively. Site 20JE67 is situated in late Cretaceous brecciated tonalites, immediately below the C-OBFZ thrust (Figure 13). The tonalites contain a set of NW-striking and SW-dipping faults of metric to decametric-scale. Fault planes contain dip-slip striations indicative of a top to-the-NE reverse movement produced under a compressional D2 regime with a N238°E trending σ_1 (Figure 12).

Site 20JE57 is located approximately 1 km to the W, just above the C-OBFZ thrust. At this site, the late Cretaceous basalts exhibit a penetrative brecciation associated with decametric-scale fault surfaces, of ENE to E strike and low/mid-dip angles to the N and S. Slip measurements establish an oblique reverse left-lateral movement on these planes. Inversion of these fault-slip data is compatible with a purely compressional D2 regime characterized by a N343°E trending σ_1 (Figure 13). Site 20JE66 is located in a nearby quarry, where basalts of the Tireo Group overthrust late Cretaceous gabbros of the Jumunuco batholith (Figure 13). Decametric-scale fault planes contain striations of contrasting kinematics: reverse dip-slip vectors in ENE to ESE-trending and N-dipping faults; oblique reverse right-lateral vectors in NNW-striking strike-slip faults; and left-lateral vectors in NE-striking strike-slip faults. Inversion of the whole striae set yields a compressional stress regime characterized by a N359°E trending σ_1 (Figure 13). Site 20JE65 is located 3 km west of Manabao village, near the link between W and C-OBFZ segments (Figure 13). At this point, basalts are intensely brecciated by a system of NE to E-striking and high-dipping faults. Slip measurements in these fault planes indicates a predominance of oblique reverse left-lateral slip movement compatible with a purely compressional D2 regime with a N027°E trending σ_1 (Figure 13).

5. Discussion

5.1. Evolution of the Quaternary Stress Tensor in Southern Central Hispaniola

Based on the geometric characteristics of the faults at all scales, the movement vectors in their planes and the obtained stress tensors, three types of fault kinematics have been found in southern central Hispaniola: reverse faulting with horizontal σ_1 and σ_2, strike-slip faulting with horizontal σ_1 and σ_2, and normal faulting with vertical σ_1 (Figure 14). Therefore, since at one location two different stress tensors cannot exist contemporaneously, more than one deformation event must be considered. Different deformation events have also been distinguished

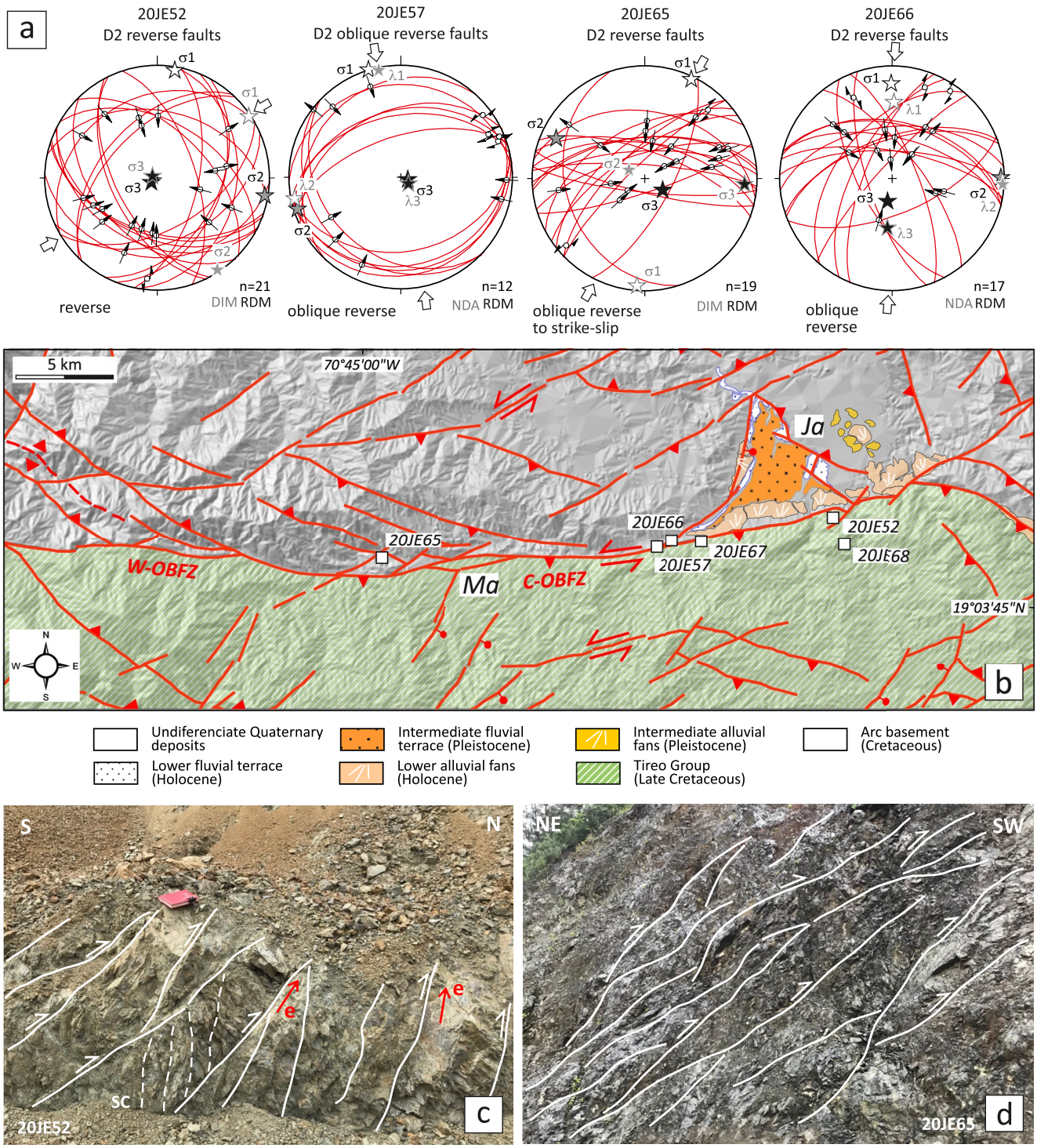

Figure 13. Structural analysis of W and C-OBFZ segments. (a) Stereoplots of the principal stress-axes obtained from inversion of fault-slip data (see Supporting Information S3 and S4). (b) Structural map of the W and C-OBFZ segments and the Quaternary Jarabacoa basin. Ja, Jarabacoa; Ma, Manabao. (c) Basalts and pyroclastic rocks of the Tireo Group deformed by D2 reverse faults related to the N-directed C-OBFZ thrust. Note the high-pitch angle of the striations [e] on the fault planes. (d) Basalts of the Tireo Group intensely brecciated by a system of high-angle D2 thrust faults related to the C-OBFZ.

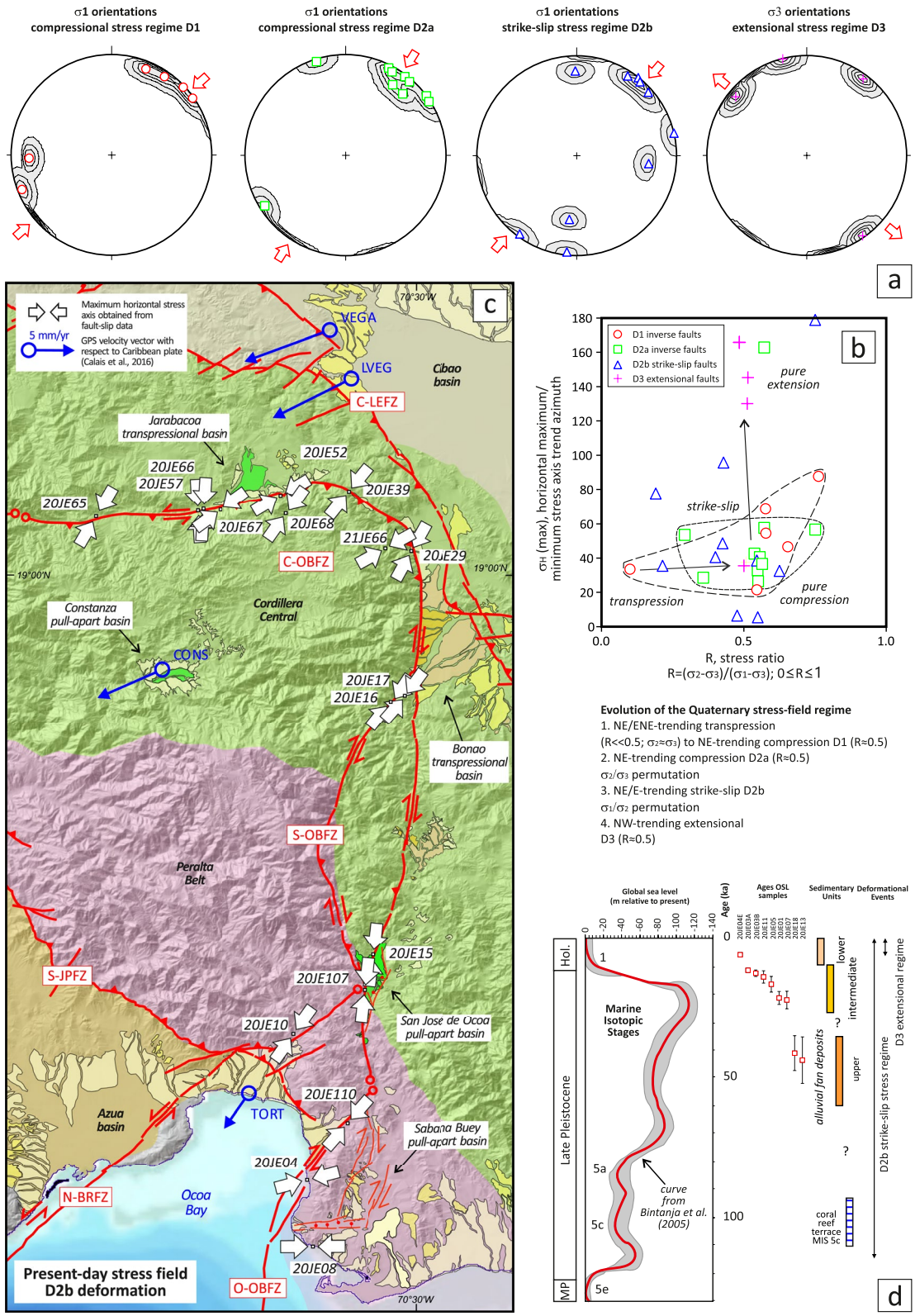

Figure 14.

through field crosscutting relations between faults of contrasting geometry and kinematics, as well as offset relations with dated lithostratigraphic units. This section discusses these evens from the oldest to the youngest.

Evidence for a NE to ENE-trending compression D1 stress regime is recorded throughout the southern Cordillera Central by slip on thrust and reverse faults that affect the Oligocene-lower Miocene Río Ocoa Group rocks, the early Miocene-middle Pliocene turbiditic and marine platform sediments of the Azua basin, and the late Pliocene-Early Pleistocene coarse-grained clastic continental deposits of the Arroyo Seco Fm. As previously reported by Heubeck and Mann (1991), Hernáiz-Huerta and Pérez-Estaún (2002) and Pérez-Valera (2010), among others, the D1 deformation took place during the fold-and-thrust belt development above a basal detachment horizon following a forward propagating sequence to the SW.

Stress tensors obtained for D1 event indicate a general NE-trending σ_1 axis, ranging between N022°E and N088°E directions, with a relatively well-constrained maximum value in the count contours stereoplot at N051°E, plunging 01° to the NE (Figure 14). In this calculation, the orientation of σ_1 has been restored at sites that have undergone a post-D1 clockwise rotation. The vertical arrangement of σ_3 axis is consistent with deformation by thrusting. The stress ratio R has values close to 0.50 that indicate stress tensors close to pure compression. Therefore, the regional D1 stress regime consisted of a NE-trending subhorizontal compression. However, the $R = 0.10$ value obtained punctually (21JE107A), which means that the minimum σ_H axis is close in magnitude to σ_V ($\sigma_2 \approx \sigma_3$), suggests that a transpressional regime locally characterizes the D1 deformation. Since D1 structures are recorded in the Arroyo Seco Fm and older rock units, the D1 stress-field is representative of pre-Early Pleistocene times.

From a geometric point of view, D2 structures were separated into D2a and D2b events. The NE-trending compressional D2a stress regime is only observed in the vicinity of the OBFZ, particularly in the eastern sector of the Ocoa Bay and the margins of the San José de Ocoa basin. E to NE-verging back-fold and back-thrust D2a structures deform the Arroyo Seco Fm, as well as older rocks. However, no D2a structures are observed affecting the fossil coral reef terrace formed during the MIS 5c stage (~100–110 ka), nor the overlying continental alluvial fan deposits. Thus, the D2a stress regime is younger than the D1 deformation, only recorded in pre-Early Pleistocene sedimentary units, and older than MIS 5c stage (boundary between the Middle and Late Pleistocene). D2a stress tensors indicate a general NE-trending σ_1 axis, ranging between N029°E and N058°E, and a subvertical σ_3 axis. The well-constrained máximum value in the stereoplot of σ_1 axes is N032°E, plunging 06° to the NE, including data from sites located in the eastern Ocoa Bay restored to a pre-D2b orientation (Figure 14). Stress ratio values close to 0.5 indicate stress tensors close to pure compression.

The NE to ENE-trending strike-slip D2b stress regime is also only detected in sectors close to the OBFZ, particularly in the eastern sector of the Ocoa Bay and in the San José de Ocoa, Bonao and Jarabacoa intramountain basins. D2b strike-slip faults cut and displace the structures of the D1 fold-and-thrust belt, as already noted by Heubeck and Mann (1991), Hernáiz-Huerta and Pérez-Estaún (2002) and Pérez-Valera (2010), as well as the D2a back-thrusts. They deform the Quaternary deposits in several places, as the Late Pleistocene fluvial terraces in the Bonao (20JE18) and Jarabacoa (20JE54B) basins, and the latest Pleistocene deposits of the intermediate alluvial fan in the eastern Ocoa Bay (20JE03). As these deposits are not deformed by D2a, the D2b stress regime is therefore younger. However, D2b strike-slip faults are locally fossilized by alluvial fan deposits of Holocene age (20JE04E). On the other hand, the OBFZ and associated minor faults exhibit offsets of geomorphic features, such as late Quaternary alluvial fans and streams, which indicate that D2b deformation currently occurs through the study region.

Stress tensors of D2b event indicate a general NE-trending σ_1 axis, comprised between N006°E and N179°E directions, with a relatively well-constrained maximum value at N042°E, plunging 06° to the NE (Figure 14).

Figure 14. (a) Stereoplots of the principal stress-axes obtained from fault-slip data inversion grouped by deformation events and (b) their classification according to its kinematic regime (see Supporting Information S5). The orientation of σ_1 has been restored at sites that have undergone a post-D1 rotation. Contours in stereoplots at 1.0%, 5.0%, 10.0%, 15.0%, 20.0%, and 25.0%. Computed σ_1 (σ_3 for D3 extension) mean stress axes: D1, máximum value 25.7% at N051°E/01NE; D2a, máximum value 24.3% at N032°E/06NE; D2b, máximum value 25.3% at N042°E/06NE; and D3 máximum value 24.2% at N326°E/06NW. (c) Map of present-day horizontal maximum stress axis trend (D2b) in southern central Hispaniola derived from fault-slip data inversion. Shaded relief in grayscale has been made as in Figure 3, indicating the overlay color indicating the different geological domains: yellow, the Neogene Cibao basin; green, the Cretaceous basement of the Cordillera Central; red, the middle Eocene-lower Miocene Peralta fold-and-thrust belt and the overlying uplifted forearc basin; and orange, the Neogene Azua Basin. Acronyms as in Figures 1 and 6. Vectors of GPS velocities at stations located in the study area are from Symithe et al. (2015) and Calais et al. (2016). (d) Correlation between the chronostratigraphy, global eustatic curve of sea level, marine isotope stages (MIS), OSL geochronological results (see Supporting Information S6), Quaternary lithostatigraphic units and deformational events defined in this work over the past 130 ka. MP, Middle Pleistocene. See explanation in text.

The dispersion of σ_1 axes is due to fault-slip measures in sites located in the San José de Ocoa Basin, where the S-OBFZ trends N-S. The subvertical arrangement of the σ_2 axes indicates that the D2b deformation took place in a strike-slip regime. This regional stress regime is characterized by a NE-trending subhorizontal shortening for R-values ranging between 0.19 and 0.63. Low-R values suggest a deformation mode in some sites transitional between thrust and strike-slip faulting (i.e., transpressional), which is consistent with some focal mechanism solutions and dominance of D2b faults with oblique reverse slip vectors in these sites.

Finally, evidence of a NW-trending extensional D3 stress regime is recorded only in the southeast sector of the Ocoa Bay by slip on normal faults. These faults affect the coral reef terrace of the MIS 5c stage (20JE04) and the overlapping lower alluvial fan of Holocene age. Although the number of obtained D3 stress tensors is limited, the inversion of fault-slip data indicates a NW-trending σ_3 axis. The orientation of σ_3 axis ranges between N166°E and N052°E, with a calculated maximum value at N326°E, plunging 06° to the NW (Figure 14). Obtained R-values close to 0.5 indicate stress tensors close to pure extension. The origin of D3 faulting is poorly understood and may be attributed to local gravitational effects.

In conclusion, a relatively constant horizontal shortening of NE-SW trend, parallel to the current direction of plate convergence, controlled the evolution of the Quaternary stress tensor in southern central Hispaniola. This evolution included a D1 event of transpression/compression and a D2a event of near pure compression, which were followed by a D2b strike-slip event and locally by a D3 regime of pure extension. The successive changes in the stress regime were related to a permutation of σ_3 by σ_2 vertical stress (*sensu* Peacock et al., 2017) between D2a and D2b events, and to a permutation of σ_2 by σ_1 vertical stress between D2b and D3 events. The change from D1 to D2a compressional stress regimes took place sometime in the Early Pleistocene. This change could be related to the indentation of the Beata Ridge in southern Hispaniola, as part of the Caribbean oceanic plateau collision in the back-arc region of the Hispaniola microplate. The shift from a D2a compressional to a D2b strike-slip regimes occurred during the Early and Middle Pleistocene. This change could be related to the formation of strike-slip faults on the margins of the Beata Ridge.

5.2. Present-Day Kinematics of the Ocoa-Bonao-La Guácara Fault Zone

In southern Hispaniola, active oblique collision and underthrusting of the Caribbean oceanic plateau have imposed an external (far-) stress-field in the Gonâve and Hispaniola microplates (Hernáiz-Huerta, Díaz De Neira, García Senz, Deschamps, Lopera, et al., 2007; Hernáiz-Huerta & Pérez-Estaún, 2002; Hernáiz-Huerta & Pérez-Estaún, 2002; ; Heubeck & Mann, 1991; Mann, Draper, & Lewis, 1991, 1995; Mercier de Lépinay et al., 1988). Geodetic studies using GPS and computed strain rates establish a NNE to NE-directed compression in much of this sector (Calais et al., 2016; Mann et al., 2002; Symithe et al., 2015). Several previous studies have proposed that this external stress-field is partitioned into a parallel component accommodated by left-lateral strike-slip movement in the Enriquillo-Plantain Garden fault zone and a normal component accommodated by pure thrusting mainly at the Muertos Trough (Benford et al., 2012; Calais et al., 2002; Mann et al., 1995, 2002). In southern central Hispaniola, however, the structures that accommodate this long and short-time shorthening and the degree of deformation partitioning are poorly understood.

In this work, the geometric and kinematic analysis of neotectonic faults indicates that part of the present-day stress-field induced by the Caribbean oceanic plateau collision is accommodated by the Ocoa-Bonao-La Guacara fault zone, within the Hispaniola microplate. However, the OBFZ is a large-scale continuous structure that bends northward from a NE to a WNW trend. Given that such change in the surface geometry of the fault may result in variations in both kinematics, fault behavior and slip rate, the present-day NE-trending D2b compression is expected to be accommodated in different ways in each segment of the OBFZ.

The subhorizontal σ_1 axis trend obtained from fault-slip data inversion in D2b structures is relatively consistent throughout southern central Hispaniola and explain the kinematics of the different segments of the OBFZ (Figure 14). The general strike of the O-OBFZ is subparallel to the external NE-directed shorthening and the GPS motion measured in the TORT station (N212°E direction relative to the Caribbean plate), which implies strike-slip faulting along the fault segment. This is consistent with the observed kinematics of the D2b faults zones in the site 20JE110 and the strike-slip/compressional D2b stress regime deduced from fault-slip inversion. In this tectonic context, the E-striking Sabana Buey depression is an active pull-apart basin developed by local transtension in a 10 km-scale right-stepping releasing bend (Figure 14).

Toward the NE, the strike of the S-OBFZ forms an acute angle (~40°) with the GPS velocity vector measured in the TORT station, which implies an oblique reverse right-lateral to strike-slip faulting along the segment. This

agrees with the oblique reverse to strike-slip kinematics observed along the fault zone in the 20JE15 and 20JE107 sites, and the obtained strike-slip stress regimes. Formation of the rhomboidal San José de Ocoa basin as an active S-shaped pull-apart is related to a releasing-bend between two branches of the S-OBFZ. Interestingly, present-day movement along the S-OBFZ can explain the occurrence of the 05/09/1988 earthquake (*Mw* 5.6, depth 18 km; Figure 5 and Supporting Information S1) that indicate oblique reverse right-lateral faulting on a parallel NNE-striking nodal fault plane. The northern end of the segment is once again parallel to the external NE-directed shortening, obtaining a consistent strike-slip regime for NNE-striking D2b strike-slip faults in the 20JE16 site.

The WSW-directed motion measured in CONS, LVEG and VEGA stations is suborthogonal to the NW-SE strike of the central sector of the C-OBFZ, implying reverse faulting along the segment (Figure 14). This is consistent with the thrust kinematics and reverse stress regime obtained in the 20JE39 site. In this context, the active Bonao and Jarabacoa transpressional sedimentary basins developed in the front of the curved C-OBFZ. The obliquity (from 10° to 50°) between the strike of the segment and the regional shortening, as well as the GPS vectors, implies an overal oblique reverse faulting, right-lateral along the N-striking Bonao sector and left-lateral along the E-striking Jarabacoa sector. These predictions are consistent with the oblique reverse right-lateral kinematics of the C-OBFZ in the Bonao sector, as well as the reverse stress regime deduced from fault-slip data inversion in the 20JE29 and 21JE66 sites. Analogously, the oblique reverse left-lateral kinematics and the reverse to oblique reverse regimes obtained along the Jarabacoa sector of the C-OBFZ (sites 20JE52, 20JE57, 20JE65, 20JE66, and 20JE67) are compatible with these predictions.

On the other hand, the homogeneous trend of the present-day D2b stress-regime implies that there is no partitioning between the faults. Even if the faults have different motions, from pure dip-slip to pure strike-slip, it is only due to their orientation with respect to the external stress-field pattern.

5.3. Seismic Potential of the Ocoa-Bonao-La Guácara Fault Zone

In general, the potential earthquake faulting and the associated seismic hazard assessment depends largely on the assumption that future large earthquakes will occur in the same regions as historical events (Ordaz et al., 2014). Therefore, recognition of active fault zones and the spatio-temporal distribution of past earthquakes have been the primary sources of information used to forecast where big events will likely occur in a certain region. In this sense, the OBFZ presents a favorable orientation for (re)activation in the present-day stress-field, so (given its dimensions) it presumably constitutes a hazardous fault zone with the potential to produce damaging large earthquakes.

The fault segmentation model for the OBFZ presented for the first time in this work enables us to set the region of southern central Hispaniola that is deformed by this fault system. Although this region has been affected by several large earthquakes (see *Seismicity* section), the short period of time covered by the seismic catalog of historical events and, in particular, the low precision in their geographic location, constitute a great obstacle for the estimation of seismic hazard.

Despite this difficulty, the geometric, kinematic and structural characteristics of the OBFZ permit a preliminary evaluation of its seismic potential, which allows to consider the fault system as a source of large earthquakes in the regional seismic hazard assessment. Wells and Coppersmith (1994) established an empirical relationships between *Mw* (moment magnitude) and the surface rupture length for strike-slip faults, where the surface rupture length corresponds to between 50% and 100% of the maximum surface length of the fault. The segmented characteristics of the OBFZ permit to propose two maximum surface lengths: the total length of the fault system; and the length of each of its segments. In the first case, the reactivation of the 264 km of whole OBFZ length as a single seismogenic fault would give rise to an earthquake of maximum *Mw* 7.8. This maximum *Mw* drops to 7.6 if only the 168 km of cumulative length of the onland southern and central segments are considered. Nevertheless, the structural data presented in this work indicate that the different segments of the OBFZ have diverse geometric and kinematic characteristics, so it is unlikely that the fault system could rupture along its entire length. In the second case, if each segment of the OBFZ represents an independent seismogenic fault, the 45, 52, 68, and 96 km lengths of the respective O, S, C and W-OBFZ segments, yield earthquakes of maximum *Mw* between 7.0 and 7.2. Therefore, the OBFZ must be considered in the regional seismic hazard assessment.

5.4. Geodynamic Reconstructions for Arc-Oceanic Plateau Collision in Southern Hispaniola

GPlates V2.3 (www.gplates.org) allow us to reconstruct the relative movement between the Caribbean and North American plates in three evolutive stages from the middle-late Eocene to Present-day (Figure 15). The

10.1029/2022TC007618

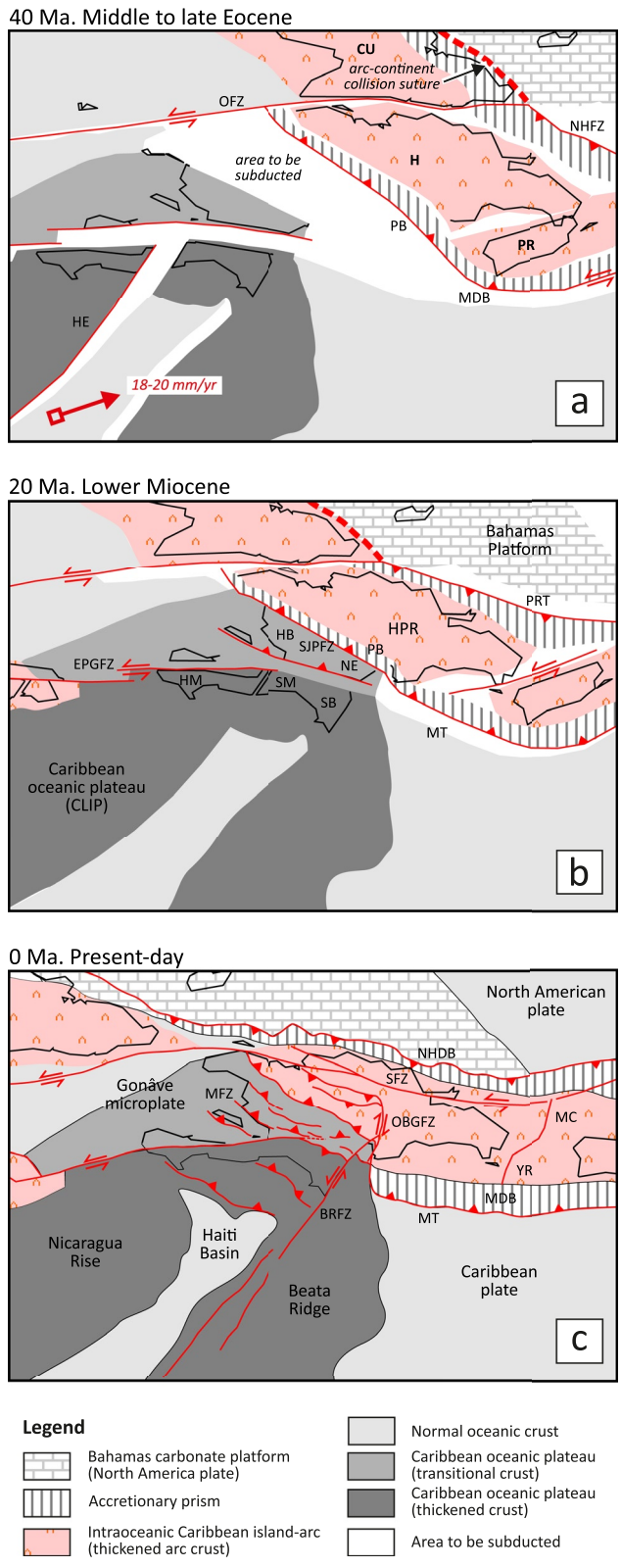

Figure 15.

diachronous collision of the early Cretaceous Caribbean island-arc with the southern continental margin of North America along a SW-dipping subduction zone ended the forward motion of the intra-oceanic arc. Arc-continent collision caused the extinction of the volcanism, the emplacement of supra-subduction zone ophiolites and the formation of a zone of NE-directed foreland thrusting on the lower plate (Escuder-Viruete, Joubert, et al., 2016; Escuder-Viruete, Súarez, et al., 2016; Mann, Draper, & Lewis, 1991; Mann, McLaughlin, and Cooper, 1991; Pérez-Estaún et al., 2007; Pindell & Kennan, 2009).

Following Kroehler et al. (2011), the suture of the arc against southern North America did not allow the subduction of more continental crust, so back-thrusting and initiation of a new SW-facing subduction zone accommodated further convergence. In Hispaniola, the terminal arc-continent collision in the middle to late Eocene (Figure 15a) resulted in a reversal of subduction polarity, as well as deformation by back-thrusting at the Peralta-Muertos accretionary prism (Dolan et al., 1991; Hernáiz-Huerta & Pérez-Estaún, 2002; Witschard & Dolan, 1990). The new subduction zone separated the Venezuela basin from the upper island-arc crust (Hispaniola-Puerto Rico microplate).

Since the lower Miocene (Figure 15b), the ENE movement of the Caribbean plate gave rise to the oblique collision/accretion of the northern sector of the Caribbean oceanic plateau of transitional crust with the Peralta Belt accretionary prism, resulting in the formation of the SW-directed Haitian-Neiba fold-and-thrust belt and the San Juan-Azua basins in the foreland (Hernáiz-Huerta & Pérez-Estaún, 2002; Pubellier et al., 2000).

During the Pliocene and until present-day, the EPGFZ is a left-lateral strike-slip fault separating the Gonâve microplate from the Caribbean plate (Calais et al., 2016; Mann, Draper, & Lewis, 1991; Mann, McLaughlin, and Cooper, 1991; Symithe et al., 2015). In this time interval (Figure 15c), deformation in the fold-and-thrust belt continues to propagate southwestward, incorporating marine to upper Pliocene-Early Pleistocene continental clastic sediments (Arroyo Seco Fm). Finally, convergence gave rise to the collision/accretion of the oceanic plateau of thickened crust, causing the uplift and folding of the Massif de la Serre-Sierra de Bahoruco and the tectonic individualization of the Enriquillo-Cul de Sac basin. Coeval to a change in the stress regime from compressional (D1) to strike-slip (D2), the OBFZ and BRFZ formed in the Pleistocene. Both fault zones delimit a submerged block of the Caribbean oceanic plateau whose indentation in southern Hispaniola produced the large-scale drag of the pre-existing structures. In this sense, the characteristics of the D2 deformation are analogous to the back-thrusts and conjugate strike-slip faults developed above of a subducted conical seamount or submarine aseismic ridge (Gardner et al., 2013; Ranero and von Huene, 2000; Sak et al., 2009), as it has been faithfully reproduced by sandbox analogue models of such convergent margins (Dominguez et al., 2000).

At a regional scale, the OBFZ connects the onshore arc-oceanic plateau collisional wedge to the offshore the Muertos accretionary wedge over a subduction zone. Thus, this fault zone defines the onland transition zone between the present-day oceanic subduction and arc-oceanic plateau collision, without any partitioning process. The OBFZ transmits also part of the compression from the collision zone further north, to the tectonic contact between the Cordillera Central and the Cibao basin.

Figure 15. Geodynamic reconstructions for the Caribbean region made with GPlates V2.3 (www.gplates.org), a global plate motion model in which the positions through time of all tectonic fragments are given digitally. (a) At 40 Ma, an area of the Caribbean plate was subducting under the back-arc of the Caribbean island-arc. NE-directed subduction started in southern Hispaniola due to previous arc-continent collision in northern Hispaniola, transfer of convergence by blocking the suture area, and subsequent back-thrusting in a large-scale restraining bend related to the opening of the Cayman Trough. Consequently, the Peralta Belt and the Muertos Trough were formed in the Hispaniola-Puerto Rico upper microplate. (b) At 20 Ma, the Enriquillo-Plantain Garden fault zone individualized the Gonâve microplate. This microplate approached the subduction zone of southern Hispaniola until the closure of the intermediate ocean. With the arc-Caribbean oceanic plateau collision, the deformation propagated to the SW, and the Haitian fold-and-thrust belt and the Sierra de Neiba-Matheaux thrust formed. (c) At present-day, further accommodation of the convergence takes place with new subduction in the Haiti Basin, the left-lateral displacement along the EPGFZ, and the indentation of the Beata Ridge between the OBFZ, which is oblique to the Muertos accretionary prism, and the BRFZ, among other structures. Therefore, the Ocoa-Bonao-La Guacara fault zone constitutes the transition between oceanic subduction and arc-oceanic plateau collision. BRFZ, Beata Ridge fault zone; Cu, Cuba; HB, Haitian fold-and-thrust belt; H, Hispaniola (Dominican Republic and Haiti); HM; Hotte Massif; MT, Muertos Trough; NE, Sierra de Neiba-Matheaux thrust; OFZ, Oriente fault zone; PB, Peralta Belt; PR, Puerto Rico; PRT, Puerto Rico Trench; SM, Serre Massif; SB, Sierra de Bahoruco. Other abbreviations as in Figure 1.

6. Conclusions

We reached the following conclusions:

1. The evolution of the Quaternary stress tensor in southern central Hispaniola was controlled by a horizontal shortening of NE-SW trend, subparallel to the current direction of plate convergence.
2. This evolution included a D1 event of transpression/compression and a D2a event of near pure compression, which were followed by a D2b strike-slip event and locally by a D3 regime of pure extension.
3. Each of these stress regimes are characterized by distinct kinematic types of faults: SW-directed thrusting and reverse faulting for D1; back-folding and back-thrusting for D2a; strike-slip to transpressional faulting for D2b; and normal faulting for D3.
4. The shift from compressional to strike-slip regimes occurred during the Early and Middle Pleistocene. This change could be related to the formation of strike-slip faults on the margins of the indenting Beata Ridge, as part of the Caribbean oceanic plateau collision in the back-arc region of the Hispaniola microplate.
5. Part of the present-day stress-field induced by the Beata Ridge collision is accommodated by the Ocoa-Bonao-La Guacara fault zone within the Hispaniola microplate. This fault zone is composed of four fault segments with different kinematics according to its orientation with respect to the ongoing NE-directed shortening.
6. The Ocoa-Bonao-La Guacara fault segments are independent seismogenic faults of several tens of kilometers long, capable of producing earthquakes of about 7.0 maximum *Mw* and transcendent in the regional seismic hazard assessment.

Data Availability Statement

The data for this paper are contained in the text, figures and supporting information and can also be found in the data repository DIGITAL.CSIC which is the institutional repository of the Spanish National Research Council (Escuder-Viruete et al., 2023).

Acknowledgments
The authors would like to thank the support and infrastructure provided by the Servicio Geológico Nacional of the Dominican Republic, particularly to Yésica Pérez-Alejandro, Maria Betania Roque-Quezada and Santiago Muñoz. We appreciated the collaboration of Marc Joubert (BRGM), Ángela Suárez and Alberto Díaz de Neira (IGME-CSIC) in early fieldwork. Detailed and constructive reviews by two anonymous reviewers, as well as the editorial work by Margaret Rusmore, significantly improved the manuscript. The research was funded through PID2019-105625RB-C22 project of the MCIN/AEI/10.13039/501100011033 of the Spanish Government.

References

Angelier, J. (1994). Fault slip analysis and paleostress reconstruction. In P. Hancock (Ed.), *Continental deformation* (pp. 53–100). Pergamon Press.

Ayala, C., García-Lobón, J. L., Escuder-Viruete, J., Rey-Moral, C., Pérez-Estaún, A., & Padín-Debén, A. (2017). High-resolution magnetic, regional gravity and petrophysical characterization of the Dominican Republic tectonic domains with special focus on the Central Cordillera. *Boletin Geologico y Minero*, *128*(3), 611–631. https://doi.org/10.21701/bolgeomin.128.3.005

Bakun, W. H., Flores, C. H., & Uri, S. (2012). Significant earthquakes on the Enriquillo fault system, Hispaniola, 1500–2010: Implications for seismic hazard. *Bulletin of the Seismological Society of America*, *102*(1), 18–30. https://doi.org/10.1785/0120110077

Benford, B., Demets, C., & Calais, E. (2012). GPS estimates of microplate motions, northern Caribbean: Evidence for a Hispaniola microplate and implications for earthquake hazard. *Geophysical Journal International*, *191*(2), 481–490. https://doi.org/10.1111/j.1365-246x.2012.05662.x

Biju-Duval, B., Bizon, G., Mascle, A., & Muller, C. (1982). Active margin processes: Field observations in southern Hispaniola. *American Association of Petroleum Geologists Memoir*, *34*, 325–344.

Calais, E., Bethoux, N., & Mercier de Lépinay, B. M. (1992). From transcurrent faulting to frontal subduction: A seismotectonic study of the northern Caribbean plate boundary from Cuba to Puerto Rico. *Tectonics*, *11*(1), 114–123. https://doi.org/10.1029/91tc02364

Calais, E., Mazabraud, Y., Mercier de Lépinay, B., Mann, P., Mattioli, G., & Jansma, P. (2002). Strain partitioning and fault slip rates in the northeastern Caribbean from GPS measurements. *Geophysical Research Letters*, *29*(18), 1856. https://doi.org/10.1029/2002gl015397

Calais, E., & Mercier de Lépinay, B. M. (1991). From transtension to transpression along the northern Caribbean plate boundary of Cuba: Implications for the recent motion of the Caribbean plate. *Tectonophysics*, *186*(3–4), 329–350. https://doi.org/10.1016/0040-1951(91)90367-2

Calais, E., Symithe, S., Mercier de Lépinay, B. M., & Prépetit, C. (2016). Plate boundary segmentation in the northeastern Caribbean from geodetic measurements and neogene geological observations. *Comptes Rendus Geoscience*, *348*(1), 42–51. https://doi.org/10.1016/j.crte.2015.10.007

Célérier, B., Etchecopar, A., Bergerat, F., Vergely, P., Arthaud, F., & Laurent, P. (2012). Inferring stress from faulting: From early concepts to inverse methods. *Tectonophysics*, *581*, 206–219. https://doi.org/10.1016/j.tecto.2012.02.009

Deschamps, Y. (2004). *Mapa Geológico de la Hoja a E. 1:50.000 nº 5871-IV (Boca Cachón)* (p. 135). Dirección General de Minería. Retrieved from https://www.sgn.gob.do

Díaz de Neira, J. A. (2000). Evolución geomorfológica del Llano de Azua (Sur de la República Dominicana). *Acta Geológica Hispánica*, *37*, 207–227.

Díaz de Neira, J. A. (2004a). *Mapa Geológico de la Hoja a E. 1:50.000 nº 5970-I (Barahona)* (p. 68). Dirección General de Minería. Retrieved from https://www.sgn.gob.do

Díaz de Neira, J. A. (2004b). Mapa Geológico de la Hoja a E. 1:50.000 nº 5971-I (Villarpando) Dirección General de Minería (p. 88). Retrieved from https://www.sgn.gob.do

Díaz de Neira, J. A., & Solé Pont, F. J. (2002). Precisiones estratigráficas sobre el Neógeno de la cuenca de Azua (República Dominicana). *Acta Geologica Hispanica*, *37*, 163–181.

Dillon, W. P., Edgar, N. T., Scanlon, K. M., & Coleman, D. F. (1996). A review of the tectonic problems or the strike-slip northern Boundary of the Caribbean plate and examination by GLORIA. In J. V. Gardner, M. E. Field, & D. C. Twichel (Eds.), *Geology of the United States seafloor: The view from GLORIA* (Vol. 9, pp. 135–164). Cambridge University Press.

Dolan, J., Mann, P., De Zoeten, R., Heubeck, C., & Shiroma, J. (1991). Sedimentologic, stratigraphic, and tectonic synthesis of Eocene-Miocene sedimentary basins, Hispaniola and Puerto Rico. In P. Mann, G. Draper, & J. F. Lewis (Eds.), *Geologic and tectonic development of the North America-Caribbean Plate boundary in Hispaniola* (Vol. 262, pp. 17–26). Geological Society of America Special Paper.

Dolan, J. F., Mullins, H. T., & Wald, D. J. (1998). Active tectonics of the north-central Caribbean region: Oblique collision, strain partitioning and opposing slabs. In J. Dolan & P. Mann (Eds.), *Active strike-slip and collisional tectonics of the northern Caribbean Plate boundary in Hispaniola* (Vol. 326, pp. 1–61). Geological Society America Special Paper.

Dominguez, S., Malavieille, J., & Lallemand, S. E. (2000). Deformation of accretionary wedges in response to seamount subduction: Insights from sandbox experiments. *Tectonics*, *19*(1), 182–196. https://doi.org/10.1029/1999tc900055

Draper, G., Mann, P., & Lewis, J. F. (1994). Hispaniola. In S. K. Donovan & T. A. Jackson (Eds.), *Caribbean geology: An introduction* (pp. 129–150). Jamaica, University of the West Indies Publishers Association.

Draper, G., & Nagle, F. (1991). Geology, structure, and tectonic development of the Río San Juan complex, northern Dominican Republic. In P. Mann, G. Draper, & J. F. Lewis (Eds.), *Geologic and tectonic development of the North American-Caribbean Plate boundary in Hispaniola* (Vol. 262, pp. 77–95). Geological Society of America Special Paper.

Driscroll, N. W., & Diebold, J. B. (1998). Deformation of the Caribbean region: One plate or two? *Geology*, *26*(11), 1043–1046.

Dürkefälden, A., Hoernle, K., Hauff, F., Wartho, J. A., van den Bogaard, P., & Werner, R. (2019). Age and geochemistry of the Beata Ridge: Primary formation during the main phase (~89 Ma) of the Caribbean large igneous province. *Lithos*, *328–329*, 69–87. https://doi.org/10.1016/j.lithos.2018.12.021

Ekström, G., Nettles, M., & Dziewónski, A. M. (2012). The global CMT project 2004–2010: Centroid-moment tensors for 13,017 earthquakes. *Physics of the Earth and Planetary Interiors*, *1–9*, 200–201. https://doi.org/10.1016/j.pepi.2012.04.002

Escuder-Viruete, J., & Baumgartner, P. O. (2014). Structural evolution and deformation kinematics of a subduction-related serpentinite-matrix mélange, Santa Elena Península, northwest Costa Rica. *Journal of Structural Geology*, *66*, 356–381. https://doi.org/10.1016/j.jsg.2014.06.003

Escuder-Viruete, J., Beranoaguirre, A., Valverde-Vaquero, P., & Mcdermott, F. (2020). Quaternary deformation and uplift of coral reef terraces produced by oblique subduction and underthrusting of the Bahama Platform below the northern Hispaniola forearc. *Tectonophysics*, *796*, 228631. https://doi.org/10.1016/j.tecto.2020.228631

Escuder-Viruete, J., Castillo-Carrión, M., & Pérez-Estaún, A. (2014). Magmatic relationships between depleted mantle harzburgites, boninitic cumulate gabbros and subduction-related tholeiitic basalts in the Puerto Plata ophiolitic complex, Dominican Republic: Implications for the birth of the Caribbean island-arc. *Lithos*, *196–197*, 261–280. https://doi.org/10.1016/j.lithos.2014.03.013

Escuder-Viruete, J., Castillo-Carrión, M., Pérez Valera, F., Valverde-Vaquero, P., Rubio Ordónez, Á., & Fernández, F. J. (2022). Reconstructing the crustal section of the intra-oceanic Caribbean island arc: Constraints from the cumulate layered gabbronorites and pyroxenites of the Rio Boba plutonic sequence, northern Dominican Republic. *Geochemistry, Geophysics, Geosystems*, *23*(2), e2021GC010101. https://doi.org/10.1029/2021gc010101

Escuder-Viruete, J., Contreras, F., Stein, G., Urien, P., Joubert, M., Ullrich, T., et al. (2006). Transpressional shearing and strike-slip partitioning in the Caribbean island arc: Fabric development, kinematics and Ar-Ar ages of syntectonic emplacement of the loma de Cabrera batholith, Dominican Republic. *Journal of Structural Geology*, *28*(8), 1496–1519. https://doi.org/10.1016/j.jsg.2006.04.003

Escuder-Viruete, J., Fernández, F. J., Pérez Valera, F., & Medialdea, A. (2023). *Present-day accommodation of Caribbean-North American oblique plate convergence through the Ocoa-Bonao-La Guacara fault zone, southern central Hispaniola: A transition zone between oceanic subduction and arc-oceanic plateau collision*. DIGITAL.CSIC repository. Retrieved from https://digital.csic.es/handle/10261/129189

Escuder-Viruete, J., Joubert, M., Abad, M., Pérez-Valera, F., & Gabites, J. (2016). The basaltic volcanism of the Dumisseau formation in the Sierra de Bahoruco, SW Dominican Republic: A record of the mantle plume-related magmatism of the Caribbean large igneous province. *Lithos*, *254–255*, 67–83. https://doi.org/10.1016/j.lithos.2016.03.013

Escuder-Viruete, J., & Pérez, Y. (2020). Neotectonic structures and stress fields associated with oblique collision and forearc sliver formation in northern Hispaniola: Implications for the seismic hazard assessment. *Tectonophysics*, *784*, 228452. https://doi.org/10.1016/j.tecto.2020.228452

Escuder-Viruete, J., & Pérez-Estaún, A. (2013). Contrasting exhumation P–T paths followed by high-P rocks in the northern Caribbean subduction–accretionary complex: Insights from the structural geology, microtextures and equilibrium assemblage diagrams. *Lithos*, *160–161*, 117–144. https://doi.org/10.1016/j.lithos.2012.11.028

Escuder-Viruete, J., Pérez-Estaún, A., Booth- Rea, G., & Valverde-Vaquero, P. (2011). Tectonometamorphic evolution of the Samaná complex, northern Hispaniola: Implications for the burial and exhumation of high-pressure rocks in a collisional accretionary wedge. *Lithos*, *125*(1–2), 190–210. https://doi.org/10.1016/j.lithos.2011.02.006

Escuder-Viruete, J., Pérez-Estaún, A., Gabites, J., & Suárez-Rodríguez, Á. (2011). Structural development of a high-pressure collisional accretionary wedge: The Samaná complex, northern Hispaniola. *Journal of Structural Geology*, *33*(5), 928–950. https://doi.org/10.1016/j.jsg.2011.02.006

Escuder-Viruete, J., Súarez, A., Gabites, J., & Pérez-Estaún, A. (2016). The imbert formation of northern Hispaniola: A tectono-sedimentary record of arc-continent collision and ophiolite emplacement in the northern Caribbean accretionary prism. *Solid Earth Discuss*, *6*, 1–50.

Escuder-Viruete, J., Valverde-Vaquero, P., Rojas-Agramonte, Y., Gabites, J., & Pérez-Estaún, A. (2013). From intra-oceanic subduction to arc accretion and arc-continent collision: Insights from the structural evolution of the Río San Juan metamorphic complex, northern Hispaniola. *Journal of Structural Geology*, *46*, 34–56. https://doi.org/10.1016/j.jsg.2012.10.008

Festa, A., Dilek, Y., Pini, G. A., Codegone, G., & Ogata, K. (2012). Mechanisms and processes of stratal disruption and mixing in the development of mélanges and broken formations: Redefining and classifying mélanges. *Tectonophysics*, *568–569*, 7–24. https://doi.org/10.1016/j.tecto.2012.05.021

García-Lobón, J. L., & Ayala, C. (2007). Cartografía geofísica de la República Dominicana: Datos de densidad, susceptibilidad magnética y magnetización remanente. *Boletin Geologico y Minero*, *118*(2), 175–194.

García Lobón, J. L., & Rey Moral, C. (2004). Magnetismo y radiación gamma natural de la República Dominicana. *Boletin Geologico y Minero*, *115*(1), 153–168.

García-Senz, J. (2004). *Mapa Geológico de la Hoja a E. 1:50.000 nº 5871-III (Jimaní)* (p. 102). Dirección General de Minería. Retrieved from https://www.sgn.gob.do

Gardner, T. W., Fisher, D. M., Morell, K. D., & Cupper, M. L. (2013). Upper-plate deformation in response to flat slab subduction inboard of the aseismic Cocos Ridge, Osa Peninsula, Costa Rica. *Lithosphere*, *5*(3), 247–264. https://doi.org/10.1130/l251.1

Genna, A. (2004). *Mapa Geológico de la Hoja a E. 1:50.000 nº 5871-II (Duvergé)* (p. 50). Dirección General de Minería. Retrieved from https://www.sgn.gob.do

Granja Bruña, J. L., Carbó-Gorosabel, a., Llanes Estrada, P., Muñoz-Martín, a., ten Brink, U. S., Gómez Ballesteros, M., et al. (2014). Morphostructure at the junction between the Beata ridge and the Greater Antilles island arc (offshore Hispaniola southern slope). *Tectonophysics*, *618*, 138–163. https://doi.org/10.1016/j.tecto.2014.02.001

Granja Bruña, J. L., ten Brink, U. S., Carbó-Gorosabel, A., Muñoz-Martín, A., & Gómez Ballesteros, M. (2009). Morphotectonics of the central Muertos thrust belt and Muertos Trough (northeastern Caribbean). *Marine Geology*, *263*(1–4), 7–33. https://doi.org/10.1016/j.margeo.2009.03.010

Hernáiz-Huerta, P. P. (2004). *Mapa Geológico de la Hoja a E. 1:50.000 nº 5871-I (La Descubierta)* (p. 102). Dirección General de Minería. Retrieved from https://www.sgn.gob.do

Hernáiz-Huerta, P. P., Díaz De Neira, J. A., García Senz, J., Deschamps, I., Genna, A., Nicole, N., et al. (2007). La estructura de la sierra de Neiba, margen norte de la sierra de Bahoruco, Sierra de Martín García y cuenca de Enriquillo de la República Dominicana: Un ejemplo de deformación transpresiva. *Boletin Geologico y Minero*, *118*, 337–357.

Hernáiz-Huerta, P. P., Díaz De Neira, J. A., García Senz, J., Deschamps, I., Lopera, E., Escuder Viruete, J., et al. (2007). La estratigrafía de la Sierra de Neiba, República Dominicana. *Boletin Geologico y Minero*, *118*, 313–336.

Hernáiz-Huerta, P. P., & Pérez-Estaún, A. (2002). Estructura del cinturón de pliegues y cabalgamientos de Peralta, República Dominicana. *Acta Geológica Hispánica*, *37*, 183–205.

Heubeck, C., Mann, E., Dolan, J., & Monechi, S. (1991). Diachronous uplift and recycling of sedimentary basins during Cenozoic tectonic transpression, northeastern Caribbean plate margin. *Sedimentary Geology*, *70*, 1–32. https://doi.org/10.1016/0037-0738(91)90063-j

Heubeck, C., & Mann, P. (1991). Structural geology and Cenozoic tectonic history of the southeastern termination of the Cordillera Central, Dominican Republic. In P. Mann, G. Draper, & J. F. Lewis (Eds.), *Geologic and tectonic development of the North America-Caribbean Plate boundary in Hispaniola*, *Geological Society of America Special Paper* (Vol. 262, pp. 315–336).

Kesler, S. E., Campbell, I. H., & Allen, C. M. (2005). Age of the Los Ranchos Formation, Dominican Republic: Timing and tectonic setting of primitive island arc volcanism in the Caribbean region. *Geological Society of America Bulletin*, *117*(7–8), 987–995. https://doi.org/10.1130/b25594.1

Krebs, M., Schertl, H. P., Maresch, W. V., & Draper, G. (2011). Mass flow in serpentinite hosted subduction channels: P–T–t path patterns of metamorphic blocks in the Rio San Juan mélange (Dominican Republic). *Journal of Asian Earth Sciences*, *42*(4), 569–595. https://doi.org/10.1016/j.jseaes.2011.01.011

Kroehler, M. E., Mann, P., Escalona, E., & Christeson, G. L. (2011). Late Cretaceous-Miocene diachronous onset of back thrusting along the South Caribbean deformed belt and its importance for understanding processes of arc collision and crustal growth. *Tectonics*, *30*(6), 1–31. https://doi.org/10.1029/2011tc002918

Ladd, J. W., Shih, T.-C., & Tsai, C. J. (1981). Cenozoic tectonics of central Hispaniola and adjacent Caribbean sea. *American Association of Petroleum Geologists Bulletin*, *65*, 466–489.

Lewis, J. F., & Draper, G. (1990). Geological and tectonic evolution of the northern Caribbean margin. In G. Dengo & J. E. Case (Eds.), *The geology of North America. The Caribbean region* (Vol. H, pp. 77–140). Geological Society of America.

Manaker, D. M., Calais, E., Freed, A. M., Ali, S. T., Przybylski, P., Mattioli, G., et al. (2008). Interseismic plate coupling and strain partitioning in the Northeastern Caribbean. *Geophysical Journal International*, *174*(3), 889–903. https://doi.org/10.1111/j.1365-246x.2008.03819.x

Mann, P. (2007). Global catalogue, classification and tectonic origins of restraining- and releasing bends on active and ancient strike-slip fault systems. In W. D. Cunningham & P. Mann (Eds.), *Tectonics of strike-slip restraining and releasing bends*, *Geological Society London Special Publications* (Vol. 290, pp. 13–142).

Mann, P., Calais, E., Ruegg, J. C., Demets, C., Jansma, P. E., & Mattioli, G. S. (2002). Oblique collision in the northeastern Caribbean from GPS measurements and geological observations. *Tectonics*, *21*(6), 1–23. https://doi.org/10.1029/2001tc001304

Mann, P., Draper, G., & Lewis, J. F. (1991). An overview of the geologic and tectonic development of Española. In P. Mann, G. Draper, & J. F. Lewis (Eds.), *Geologic and tectonic development of the North America-Caribbean Plate boundary in Española*, *Geological Society of America Special Paper* (Vol. 262, pp. 1–28).

Mann, P., McLaughlin, P. P., Jr., & Cooper, J. C. (1991). Geology of the Enriquillo-Azua basins, Dominican Republic, 2. Structure and tectonics. In P. Mann, G. Draper, & J. F. Lewis (Eds.), *Geologic and tectonic development of the North America-Caribbean plate boundary in Española*, *Geological Society of America Special Paper* (Vol. 262, pp. 367–389).

Mann, P., Prentice, C. S., Burr, G., Peña, L. R., & Taylor, F. W. (1998). Tectonic geomorphology and paleoseismology of the Septentrional fault system, Dominican Republic. In J. F. Dolan & P. Mann (Eds.), *Active strike-slip and collisonal tectonics of the Northern Caribbean plate boundary Zone*, *Geological Society of America Special Paper* (Vol. 326, pp. 63–123).

Mann, P., Taylor, F. W., Edwards, R. L., & Ku, T. L. (1995). Actively evolving microplate formation by oblique collision and sideways motion along strike-slip faults: An example from the northeastern Caribbean plate margin. *Tectonophysics*, *246*(1–3), 1–69. https://doi.org/10.1016/0040-1951(94)00268-e

Matthews, J., & Holcombe, T. (1976). Possible Caribbean underthrusting of the greater Antilles along muertos trough. In *Transactions of the 7th Caribbean geological conference* (pp. 235–242).

McLaughlin, P. P., Van Den Bold, W. A., & Mann, P. (1991). Geology of the Azua and Enriquillo basins. Dominican Republic; 1, Neogene lithofacies, biostratigraphy, biofacies, and paleogeography. In P. Mann, G. Draper, & J. F. Lewis (Eds.), *Geologic and tectonic development of the North America-Caribbean plate boundary in Hispaniola*, *Geological Society of America Special Paper* (Vol. 262, pp. 337–366).

Mercier de Lépinay, B. (1987). *L'évolution géologique de la bordure nord-caraïbe: L'exemple de la transversale del'île d'Hispaniola (Grandes Antilles)* (p. 366). Thèse d'Etat, Université Pierre et Marie Curie.

Mercier de Lépinay, B., Mauffret, A., Jany, I., Bouysse, P., Mascle, A., Renard, V., et al. (1988). Une collision oblique sur la bordure nord-Caraïbe à la jonction entre la ride de Beata et la fosse de Muertos. *Comptes Rendus de l'Académie des Sciences. Paris*, *307*, 1289–1296.

Nicol, N. (2004). *Mapa Geológico de la Hoja a E. 1:50.000 nº 5970-IV (La Salina)* (p. 135). Dirección General de Minería. Retrieved from https://www.sgn.gob.do

Ordaz, M., Cardona, O., Salgado-Gálvez, M. A., Bernal, G., Singh, K., & Zuloaga, D. (2014). Probabilistic seismic hazard assessment at global level. *International Journal of Disaster Risk Reduction*, *10*(B), 419–427. https://doi.org/10.1016/j.ijdrr.2014.05.004

Ortner, H., Reiter, F., & Acs, P. (2002). Easy handling of tectonic data: The programs TectonicVB for Mac and TectonicsFP for Window. *Computers & Geosciences*, *28*(10), 1193–1200. https://doi.org/10.1016/s0098-3004(02)00038-9

Peacock, D. C. P., Tavarnelli, E., & Anderson, M. W. (2017). Interplay between stress permutations and overpressure to cause strike-slip faulting during tectonic inversion. *Terra Nova*, *29*(1), 61–70. https://doi.org/10.1111/ter.12249

Pérez-Estaún, A., Hernaiz Huerta, P. P., Lopera, E., Joubert, M., Escuder-Viruete, J., Díaz de Neira, A., et al. (2007). Geología de la República Dominicana: De la construcción de arco-isla a la colisión arco-continente. *Boletin Geologico y Minero*, *118*, 157–174.

Pérez Valera, F. (2010). *Mapa Geológico de la Hoja a E. 1:50.000 nº 6070-I (Sabana Buey)* (p. 96). Dirección General de Minería. Retrieved from https://www.sgn.gob.do

Petit, J. (1987). Criteria for the sense of movement on fault surfaces in brittle rocks. *Journal of Structural Geology*, *9*(5–6), 597–608. https://doi.org/10.1016/0191-8141(87)90145-3

Pindell, J., & Kennan, L. (2009). Tectonic evolution of the Gulf of Mexico, Caribbean and northern south America in the mantle reference frame: An update. In K. James, M. A. Lorente, & J. Pindell (Eds.), *The geology and evolution of the region between North and South America*, *Geological Society of London Special Publication* (Vol. 328, pp. 1–55).

Prentice, C. S., Mann, P., Crone, A. J., Gold, R. D., Hudnut, K. W., Briggs, R. W., et al. (2010). Seismic hazard of the Enriquillo–Plantain Garden fault in Haiti inferred from palaeoseismology. *Nature Geoscience*, *3*(11), 789–793. https://doi.org/10.1038/ngeo991

Prentice, C. S., Mann, P., Peña, L. R., & Burr, G. (2003). Slip rate and earthquake recurrence along the central Septentrional fault, North American-Caribbean plate boundary, Dominican Republic. *Journal of Geophysical Research*, *108*(B3), 2149. https://doi.org/10.1029/2001JB000442

Pubellier, M., Mauffret, A., Leroy, S., Vila, J. M., & Amilcar, H. (2000). Plate boundary readjustment in oblique convergence: Example of the Neogene of Hispaniola, greater Antilles. *Tectonics*, *19*(4), 630–648. https://doi.org/10.1029/2000tc900007

Ranero, C. R., & von Huene, R. (2000). Subduction erosion along the Middle America convergent margin. *Nature*, *404*(6779), 748–752. https://doi.org/10.1038/35008046

Reiter, F., & Acs, P. (2000). *TectonicsFP 1.6* (p. 48). Computer Software for Structural Geology.

Révillon, S., Hallot, E., Arndt, N., Chauvel, C., & Duncan, R. A. (2000). A complex history for the Caribbean Plateau: Petrology, geochemistry, and geochronology of the beata ridge, South Hispaniola. *The Journal of Geology*, *108*(6), 641–661. https://doi.org/10.1086/317953

Rodriguez, J., Havskov, J., Botter Sorebseb, M., & Santos, L. F. (2018). Seismotectonics of south-west Dominican Republic using recent data. *Journal of Seismology*, *22*(4), 883–896. https://doi.org/10.1007/s10950-018-9738-9

Rodríguez-Zurrunero, A., Granja-Bruña, J. L., Carbó-Gorosabel, A., Muñoz-Martín, A., Gorosabel-Araus, J. M., Gómez de la Peña, L., et al. (2019). Submarine morpho-structure and active processes along the North American-Caribbean plate boundary (Dominican Republic sector). *Marine Geology*, *407*, 121–147. https://doi.org/10.1016/j.margeo.2018.10.010

Ryan, W. B. F., Carbotte, S. M., Coplan, J., O'Hara, S., Melkonian, A., Arko, R., et al. (2009). Global Multi-Resolution Topography (GMRT) synthesis data set. *Geochemistry, Geophysics, Geosystems*, *10*(3), Q03014. https://doi.org/10.1029/2008GC002332

Sak, P. B., Fisher, D. M., Gardner, T. W., Marshall, J. S., & LaFemina, P. C. (2009). Rough crust subduction, forearc kinematics, and Quaternary uplift rates, Costa Rican segment of the Middle American Trench. *Geologival Society America Bulletin*, *121*(7–8), 992–1012. https://doi.org/10.1130/b26237.1

Sen, G., Hickey-Vargas, D. G., Waggoner, F., & Maurrasse, F. (1988). Geochemistry of basalts from the Dumisseau formation. Southern Haiti: Implications for the origin of the Caribbean sea crust. *Earth and Planetary Science Letters*, *87*(4), 423–437. https://doi.org/10.1016/0012-821x(88)90006-4

Sinton, C. W., Duncan, R. A., Storey, M., Lewis, J., & Estrada, J. J. (1998). An oceanic flood basalt province within the Caribbean plate. *Earth and Planetary Science Letters*, *155*(3–4), 221–235. https://doi.org/10.1016/s0012-821x(97)00214-8

Symithe, S., Calais, E., de Chabalier, J. B., Robertson, R., & Higgins, M. (2015). Current block motions and strain accumulation on active faults in the Caribbean. *Journal of Geophysical Research: Solid Earth*, *120*(5), 3748–3774. https://doi.org/10.1002/2014jb011779

ten Brink, U. S., Bakun, W. H., & Flores, C. H. (2011). Historical perspective on seismic hazard to Hispaniola and the northeast Caribbean region. *Journal of Geophysical Research*, *116*(B12), B12318. https://doi.org/10.1029/2011jb008497

Terrier-Sedan, M., & Bertil, D. (2021). Active fault characterization and seismotectonic zoning of the Hispaniola Island. *Journal of Seismology*, *25*(2), 499–520. https://doi.org/10.1007/s10950-021-09985-0

Twiss, R. J., & Unruh, J. R. (1998). Analysis of fault slip inversions: Do they constrain stress or strain rate? *Journal of Geophysical Research*, *103*(6), 12205–12222. https://doi.org/10.1029/98jb00612

van Benthem, S., Govers, R., Spakman, W., & Wortel, R. (2013). Tectonic evolution and mantle structure of the Caribbean. *Journal of Geophysical Research: Solid Earth*, *118*(6), 3019–3036. https://doi.org/10.1002/jgrb.50235

Wells, D. L., & Coppersmith, K. J. (1994). New empirical relationships among magnitude, rupture length, rupture width, rupture area, and surface displacement. *Bulletin of the Seismological Society of America*, *84*, 974–1002.

Witschard, M., & Dolan, J. F. (1990). Contrasting structural styles in siliciclastic and carbonate rocks of an offscraped sequence: The Peralta accretionary prism, Hispaniola. *Geological Society of America Bulletin*, *102*(6), 792–806. https://doi.org/10.1130/0016-7606(1990)102<0792:cssisa>2.3.co;2